The dynamics of diluted bitumen derived oil-mineral aggregates, Part II.

Casey M. O'Laughlin, Brent A. Law, Vanessa S. Zions, Thomas L. King, Brian Robinson, Yongsheng Wu

Science Branch
Fisheries and Oceans Canada
P.O. Box 1006
1 Challenger Drive
Dartmouth NS Canada B2Y 4A2

2017

Canadian Technical Report of
Fisheries and Aquatic Sciences No. 3209

Fisheries and Oceans Canada
Pêches et Océans Canada

Canada

Canadian Manuscript Report of Fisheries and Aquatic Sciences

Manuscript reports contain scientific and technical information that contributes to existing knowledge but which deals with national or regional problems. Distribution is restricted to institutions or individuals located in particular regions of Canada. However, no restriction is placed on subject matter, and the series reflects the broad interests and policies of Fisheries and Oceans Canada, namely, fisheries and aquatic sciences.

Manuscript reports may be cited as full publications. The correct citation appears above the abstract of each report. Each report is abstracted in the data base *Aquatic Sciences and Fisheries Abstracts*.

Manuscript reports are produced regionally but are numbered nationally. Requests for individual reports will be filled by the issuing establishment listed on the front cover and title page.

Numbers 1-900 in this series were issued as Manuscript Reports (Biological Series) of the Biological Board of Canada, and subsequent to 1937 when the name of the Board was changed by Act of Parliament, as Manuscript Reports (Biological Series) of the Fisheries Research Board of Canada. Numbers 1426 - 1550 were issued as Department of Fisheries and Environment, Fisheries and Marine Service Manuscript Reports. The current series name was changed with report number 1551.

Rapport manuscrit canadien des sciences halieutiques et aquatiques

Les rapports manuscrits contiennent des renseignements scientifiques et techniques qui constituent une contribution aux connaissances actuelles, mais qui traitent de problèmes nationaux ou régionaux. La distribution en est limitée aux organismes et aux personnes de régions particulières du Canada. II n'y a aucune restriction quant au sujet; de fait, la série reflète la vaste gamme des intérêts et des politiques de Pêches et Océans Canada, c'est-à-dire les sciences halieutiques et aquatiques.

Les rapports manuscrits peuvent être cités comme des publications à part entière. Le titre exact figure au-dessus du résumé de chaque rapport. Les rapports manuscrits sont résumés dans la base de données *Résumés des sciences aquatiques et halieutiques.*

Les rapports manuscrits sont produits à l'échelon régional, mais numérotés à l'échelon national. Les demandes de rapports seront satisfaites par l'établissement auteur dont le nom figure sur la couverture et la page du titre.

Les numéros 1 à 900 de cette série ont été publiés à titre de Manuscrits (série biologique) de l'Office de biologie du Canada, et après le changement de la désignation de cet organisme par décret du Parlement, en 1937, ont été classés comme Manuscrits (série biologique) de l'Office des recherches sur les pêcheries du Canada. Les numéros 901 à 1425 ont été publiés à titre de Rapports manuscrits de l'Office des recherches sur les pêcheries du Canada. Les numéros 1426 à 1550 sont parus à titre de Rapports manuscrits du Service des pêches et de la mer, ministère des Pêches et de l'Environnement. Le nom actuel de la série a été établi lors de la parution du numéro 1551.

Canadian Technical Report of
Fisheries and Aquatic Sciences No.3209

2017

The dynamics of diluted bitumen derived oil mineral aggregates, Part II.

by

Casey M. O'Laughlin[1], Brent A. Law[1], Vanessa S. Zions[1], Thomas L. King[2], Brian Robinson[2], Yongsheng Wu[1]

[1]Coastal Ecosystem Science Division
Science Branch
Fisheries and Oceans Canada
P.O. Box 1006
1 Challenger Drive
Dartmouth NS Canada B2Y 4A2

[2]Center for Offshore Oil, Gas and Energy Research
Fisheries and Oceans Canada
P.O. Box 1006
1 Challenger Drive
Dartmouth NS Canada B2Y 4A2

Cat. No. Fs 97-6/3209E-PDF ISBN 978-0-660-08125-0 ISSN 1488-5379 (online)

Correct citation for this publication:

O'Laughlin, C., Law, B.A., Zions, V.S., King, T.L., Robinson, B. and Wu, Y. 2017. The dynamics of diluted bitumen derived oil-mineral aggregates, Part II. Can. Tech. Rep. Fish. Aquat. Sci. 3209: viii + 49p.

CONTENTS

LIST OF TABLES

LIST OF FIGURES

ABSTRACT

O'Laughlin, C., Law, B.A., Zions, V.S., King, T.L., Robinson, B. and Wu, Y. 2017. The dynamics of diluted bitumen derived oil-mineral aggregates, Part II. Can. Tech. Rep. Fish. Aquat. Sci. 3209: viii + 49p.

The export of Canadian petroleum products to international markets introduces the substantial risk of oil spills in near-shore and coastal environments. This requires a marine science perspective in response techniques and protocols, including the development of predictive models to anticipate the fate of oil spilled in the aquatic environment. The formation dynamics of oil-mineral aggregates (OMA) derived from spilled diluted bitumen remain poorly understood, and the size, settling velocity and bulk density of these particles represent valuable and sought-after components of predictive models. This report presents results from a series of low sediment concentration (15 $mg \cdot l^{-1}$), warmer water (> 10°C) wave tank experiments designed to facilitate in situ formation of OMA and measure variability in size, settling velocity and density in response to bitumen type, sediment concentration and the presence or absence of chemical dispersant. High-resolution images of settling particles were captured and analyzed for particle size and settling velocity. Oil droplet size, the rate of particle clearance from the water column, and possible effects of chemical dispersant on natural sediment flocculation are discussed. Results are compared with those of a recently published companion report characterizing previous colder water (< 10°C) experiments.

RÉSUMÉ

O'Laughlin, C., Law, B.A., Zions, V.S., King, T.L., Robinson, B. and Wu, Y. 2017. The dynamics of diluted bitumen derived oil-mineral aggregates, Part II. Can. Tech. Rep. Fish. Aquat. Sci. 3209: viii + 49p.

L'exportation des produits pétroliers canadiens vers les marchés internationaux présente un risque important de déversements de pétrole dans les milieux riverains et littoraux. Une perspective océanographique est nécessaire pour établir des protocoles et des techniques d'intervention, y compris l'élaboration de modèles de prévision afin d'être en mesure de prédire ce qui va en devenir des déversements de pétrole dans l'environnement aquatique. La formation dynamique des agrégats pétrole-minéral découlant des déversements de bitume dilué est encore mal comprise, et la taille, la vitesse de sédimentation et la masse volumique apparente de ces particules représentent des composantes précieuses et convoitées pour les modèles de prévision. Ce rapport présente les résultats d'une série d'expériences effectuées dans des réservoirs d'eau plus chaude (> 10 °C) à faible concentration de sédiments (15 $mg\ L^{-1}$). Ces expériences ont été conçues pour assurer la formation sur place des agrégats pétrole-minéral et pour mesurer la variabilité de la taille, de la vitesse de sédimentation et de la densité en fonction du type de bitume, de la concentration des sédiments et de l'absence d'agents dispersants chimiques. Des images à haute résolution de la sédimentation de particules ont été recueillies et analysées pour mesurer la vitesse de sédimentation et la taille des particules. La taille des gouttelettes d'hydrocarbures, le taux d'élimination des particules dans la colonne d'eau et les effets possibles des agents dispersants chimiques sur la floculation des sédiments naturels font tous l'objet de discussion. Les résultats sont comparés à ceux d'un rapport complémentaire récemment publié caractérisant des expériences précédentes dans l'eau plus froide (< 10 °C).

PREFACE

The following technical report, '*The dynamics of diluted bitumen derived oil-mineral aggregates, Part II*' is a continuation of an assemblage of data generated through a series of experiments in the wave tank facility operated by the Centre for Offshore Oil, Gas and Energy Research (COOGER) at Bedford Institute of Oceanography. The reported series of experiments were completed in April to October 2014.

Experiments summarized and discussed herein comprise the low sediment concentration (15 $mg \cdot l^{-1}$), warm water (>10°C) portion of wave tank testing. Also included is a general comparison with colder water (<10°C) experiments described in *Part I* of this work. Further testing will be reported to describe high sediment concentration (50 $mg \cdot l^{-1}$) conditions with colder and warmer water.

This report is a product of the Particle Dynamics Lab at Bedford Institute of Oceanography, in Dartmouth, Nova Scotia.

1.0 INTRODUCTION

1.1 INITIATIVE

The Ocean Protection Plan is a Government of Canada initiative designed to improve marine safety and protect Canada's marine environment, including improvements to the operating environment of the oil transport industry through development and refinement of responsiveness to marine oil spills. The program is driven by the potential export of Alberta crude oil to international markets (Government of Canada, 2013). Proposed pipeline projects will move diluted bitumen to coastal areas where the material will be loaded onto marine oil tankers and shipped internationally. This introduces a substantial risk of possible oil spills in near-shore and coastal environments, and requires an oceanographic perspective in the development of response techniques and protocols.

1.2 BACKGROUND

Flocculation, or the clustering of discrete particles into loosely-packed aggregates, strongly influences the settling and subsequent deposition of fine-grained suspended particles in the marine environment (Kranck, 1973; McCave, 1984; Kranck and Milligan 1985; Kranck and Milligan 1992). A flocculated suspension represents a balance between forces that encourage floc growth through inter-particle encounters, such as particle adhesion properties and the concentration of suspended particles, versus the turbulent shear forces that pull flocs apart (Manning and Dyer, 2002; Milligan and Law, 2005). As flocs form, they increase in size, and as a result settle faster than their constituent particles (Sternberg *et al.*, 1999; Curran *et al.*, 2007). With increasing flocculation efficiency, the flux of fine-grained material to the seabed increases as well. This has been shown to facilitate rapid clearance of the water column, and can quickly result in large amounts of fine sediment deposition (Milligan *et al.*, 2007). Generally speaking, it is understood that the majority of fine-grained sediment found on the seabed is deposited within flocs (Kranck, 1980; Curran *et al.*, 2002). Flocculation is therefore a key element of complex sediment transport-hydrodynamic models, which combine the multiple forces at work to determine the potential fate of fine-sediment particles in near-shore and coastal zones. Similar predictive modelling methods are used to evaluate the fate of oil spilled in the marine environment (e.g. Niu *et al.*, 2011, 2012; Gong *et al.*, 2014; Zhao *et al.*, 2016a). Models designed for this purpose must incorporate parameters related to the dynamics of spilled oil, such as the formation of oil-mineral aggregates (OMAs). Similar to flocculation, the formation of OMAs is a result of inter-particle collisions and is largely influenced by the presence and concentration of suspended particulate matter (SPM) and the level of mixing energy

available (Khelifa *et al.*, 2005; Li *et al.*, 2007, 2009; Sun *et al.*, 2013). OMAs can develop as portions of surface oil slicks are broken down - by wave action, tidal mixing or chemical dispersants – to produce discrete oil droplets. In the presence of sufficient amounts of fine-grained sediment, these droplets can become coated in micron-scale particles, forming a sediment layer around oil droplets. This increases droplet stability and reduces stickiness, preventing droplets from coalescing and decreasing their adherence to surfaces in the coastal zone (Page *et al.*, 2000; Lee *et al.*, 2003; Zhao *et al.*, 2016). As oil droplets become covered in a layer of fine sediment, particle density increases and eventually, they can sink (Owens, 1999). The widespread impacts of spilled oil can be reduced by OMA formation and subsequent oil mobility (Khelifa *et al.*, 2008 a,b; Owens, 1999). From a spill management perspective, rather than sedimentation, the ideal circumstance for oil droplets that are shed from a slick is the formation of neutrally buoyant OMAs that sink slowly in the water column, where rates of biodegradation by organisms are enhanced (Venosa and Holder, 2007; Lindstrom and Braddock, 2002). Recent work suggests that the sinking rate of OMAs is primarily influenced by the density of oil, water and sediment, as well as parameters that affect oil droplet size distribution (Wu *et al.*, 2016).

Previous research has shown that most OMA formation occurs at or above a sediment concentration of 50 $mg \cdot L^{-1}$ and is linked to the presence of sufficient amounts of fine sediment particles (Khelifa *et al.*, 2008b; Ajijolaiya *et al.*, 2006). A critical sediment concentration for maximized OMA formation, identified by Ajijolaiya *et al.* (2006), was found to increase linearly with particle size (ranging from 200 $mg \cdot L^{-1}$ for 1 μm particles to 490 $mg \cdot L^{-1}$ for 16 μm particles). However, it has also been shown that increasing the mineral concentration beyond 100 $mg \cdot L^{-1}$ does not translate to an appreciable increase in the trapping efficiency of fine-grained sediments (Sun *et al.*, 2013). Other factors relevant to OMA formation include oil viscosity (Khelifa *et al.*, 2002; 2007), the hydrophobicity of minerals (Zhang *et al.*, 2010), the effects of salinity and sediment type (Khelifa *et al.*, 2005), and other sedimentary properties (Wang *et al.*, 2011). During oil spill response countermeasures, the use of chemical dispersants (e.g. Corexit®EC-9500A) has been shown to be the dominant influence on the formation and behaviour of OMA (Zhang *et al.*, 2010; Lee *et al.*, 2008). Dispersant chemically breaks down oil slicks by reducing oil-water interfacial tension, facilitating a decrease in oil and OMA droplet size distribution. This accelerates and increases the overall transfer of oil from the surface downward into the water column, compared with instances of natural dispersion (Li *et al.*, 2007; 2008). However, the potential coalescence of dispersed oil particles has been demonstrated, and this may lead to droplets floating back to the water surface (Zhang *et al.*, 2010). This notion is supported by recent research suggesting that the application of chemical dispersant alone is not as effective at distributing oil into the water column as applying dispersant in the presence of sufficient amounts of mineral fines (King *et al.*, 2015).

Studies on the transport and fate of OMA are becoming increasingly common, but are still in need of refinement and validation (Niu *et al.*, 2011; Gong *et al.*, 2014). This makes studies modelling the formation and behaviour of OMAs increasingly relevant (e.g. Hill *et al.*, 2002; Sun *et al.*, 2013; Sun *et al.*, 2014). Furthermore, diluted bitumen, or dilbit, has been largely excluded from previous efforts to determine the behaviour and fate of oil particles in the marine environment, with the exception of recently emerging research (e.g. Government of Canada, 2013; King *et al.*, 2014, 2015; O'Laughlin *et al.*, 2016). Dilbit is a combination of lighter diluents and heavy bitumen oil, produced with the goal of lowering the material's density and viscosity for transport. It has been shown that dilbit is capable of forming OMA and sinking in freshwater conditions (Lee *et al.*, 2012), and that the chemical composition of various dilbit products has an influence on fate and behaviour in the marine environment (King *et al.*, 2014). However, a recent Government of Canada report (2013) identified knowledge gaps regarding the exact conditions which allow dilbit to sink in the marine environment. It is therefore highly desirable to expand this knowledge toward a thorough understanding of fate and behaviour of dilbit released into the marine environment.

Wave tank experiments described here and in companion reports were designed to investigate the interaction of fine sediment with diluted bitumen products, in the presence and absence of chemical dispersants. The overall goal of this research is to measure variability in particle size and settling velocity of *in situ* formed OMA, in response to changes in: (1) suspended sediment concentration, (2) the presence of chemical dispersants, and (3) the type of oil. This was completed through large-scale wave tank experiments designed to replicate the natural formation of OMA. This report presents data from 15 $mg \cdot L^{-1}$, warmer water experiments (> 10 °C), and accompanies recently published 15 $mg \cdot L^{-1}$, colder water (< 10 °C) results. Future work will consider 50 $mg \cdot L^{-1}$ sediment over a similar range of water temperatures and salinity conditions. Ultimately, transport parameters derived from this research will be applied in predictive modelling studies on the transport and fate of OMA in the environment, including the particle size distribution and settling velocity of dilbit-derived OMA.

2.0 METHODOLOGY

2.1 GENERAL APPROACH

This report presents results and analysis of 16 low sediment concentration (15 $mg \cdot L^{-1}$) wave tank experiments (Table 1). Experiments were designed to simulate *in situ* conditions for OMA formation in the marine environment in the presence of regular, breaking waves. This work provides opportunities for measurements of OMA particle size and settling velocity as well as estimates of particle density, under changing

experimental conditions including the type of oil, water temperature and the presence or absence of chemical dispersant. Eight warm water experiments (> 10°C), grouped into dispersed and non-dispersed categories, are the main subject of this report (Table 1).

2.2 WAVE TANK DATA COLLECTION

Experiments in the wave tank facility operated by the Centre for Offshore Oil, Gas and Energy Research (COOGER) at the Bedford Institute of Oceanography began in April 2014. Experiments were conducted using dispersed and non-dispersed samples of weathered Access Western Blend (12 experiments) and Cold Lake Blend (6 experiments) diluted bitumen (Table 1). Two additional experiments were completed using sediment only, with no oil or dispersant (not shown in Table 1). Both dilbit products were artificially weathered by approximately 7-9% so as to simulate oil properties that would be encountered by first responders during an actual spill. The physical properties of these oils can be found in Table 2. The sediment component used was fine-grained material from two locations in Douglas Channel (British Columbia, Canada). Sediment from this particular location was selected for wave tank experiments in response to the proposed Northern Gateway pipeline initiative, which would involve tanker traffic carrying petroleum products through Douglas Channel. Approximately 1 kilogram of sediment was added to the wave tank, dependant on the sediment moisture content, to achieve a sediment concentration of ~15 $mg \cdot L^{-1}$. When dispersant was applied, Corexit®EC-9500A was used, at a dispersant-to-oil ratio (DOR) of 1:20. Oil was added to the tank by pouring into a 45 cm diameter containment ring located 10 meters downstream from the wave paddle (Figure 1). The oil was heated to 30°C to aid in the pouring process, although this heat quickly dissipated once the oil hit the water. Dispersant was sprayed on top of the slick using a commercial paint sprayer. The containment ring was removed once the first breaking wave was generated and the oil gradually distributed throughout the tank. Addition of oil and dispersant took approximately five minutes, during which time waves were shut off.

The wave tank facility is composed of a 40-meter long tank, measuring 2 m deep and 60 cm wide (Figure 1). An average water level in the tank of 1.5 meters was maintained throughout experiments. The computer-controlled wave-generating paddle is located 1 meter from the front end of the tank. During wave production, each wave train lasts approximately 15 seconds and includes a set of 3 breaking waves, followed by 25 seconds of quiescence. Maximum wave amplitude was 22.5 cm. To minimize wave reflection, energy is absorbed at the back of the tank by a series of screens. This system is designed to simulate the propagation and breaking of deep-water waves, based on linear wave theory (Li *et al.*, 2007; 2008). Each wave tank experiment was composed of four 1-hour phases: (1) mixing ‘A’ (sediment only), (2) mixing ‘B’ (sediment, oil), (3) settling and (4) flushing. Just prior to experiments, Bedford Basin

seawater was pumped into the wave tank and filtered at 5 μm to limit sediment fines and particulate organic material. Sediment was added, and waves generated for a total of 2 hours during mixing phases. Following 1 hour of sediment mixing, oil (and dispersant, when required) was added to the tank, followed by another hour of mixing. Waves were then turned off during the 1-hour settling phase.

High-resolution images (3296 x 2472 pixels; 93.8 pixels/mm) of suspended and settling particles were collected over the duration of wave tank experiments, with two machine-vision floc cameras (MVFC) (model Prosilica GX3300 from Allied Vision, 8.0 megapixel), with measurement ranges of 45 μm to ~4 cm. One camera was positioned approximately 10 meters from the wave generating paddle, with the sampling volume at 35 cm below the surface (position 'B', Figure 1), and captured one image every 30 seconds. This camera was co-located with a LISST 100-X (type C), which sampled every 3 seconds over a measurement range of 2.5 to 500 μm. Together, these datasets cover the full range of anticipated particle sizes. The velocity of settling particles was measured with a second, further-specialized floc camera, known as the size versus settling MVFC (SVS-MVFC). This instrument is equipped with a rectangular settling column (50×10×5 cm) with baffled top above the field of view. During each wave tank experiment, this camera acquired a continuous (at 11 frames per second) 30-second stream of images at 5-minute intervals. During wave tank experiments, the SVS-MVFC was placed on the bottom of the tank, 17.5 meters from the paddle (~2/3 of the tank length) (position 'D', Figure 1), with the baffled top through which particles fall at 80 cm depth, and the sampling volume at 130 cm depth.

Image analysis to derive particle size and size versus settling relationships was completed in MATLAB. Raw image files were converted to greyscale bitmaps and thresholded using ImageJ (Schneider *et al.*, 2012). The threshold grayscale value, which is used to differentiate particle edges from the background, was defined using Otsu's method for SVS-MVFC images, and the triangle method for MFVC images (Mikkelsen *et al.*, 2007b; Fox *et al.*, 2004). Grain size statistics (particle area, shape descriptors, diameter, and perimeter) were calculated, and particle size spectra derived from MVFC images were binned to compliment LISST data. Particle size data generated from the MFVC (> 45 μm) were manually merged with that of the LISST (2.5 – 500 μm) to produce continuous grain size spectra covering a size range of 2.5 μm to centimeter-scale. Merging began at the 63 μm bin, where the resultant value is derived from 50% LISST data and 50% MFVC data. From there, the ratio of value contributions from each dataset is changed in 10% increments per bin (e.g. 60-40, 70-30, etc), in favor of the dataset with the appropriate size range. The resulting merge of camera and LISST datasets occurs over nine size bins. These data are herein referred to as merged particle size spectra, cover a range of 45 μm up to several millimeters, and are plotted as the log of particle diameter (μm) versus the log of volume concentration

(ppm) or the log of equivalent weight (%). Size-settling velocity relationships and particle density estimates were developed from images collected with the SVS-MVFC. Four frames, each separated by one second in time, were overlain to produce a single, composite image. This was used to derive continuous tracks for individual particles across the sensing zone. Particles from each frame were numbered and color-coded in composite images, which allows individual particles to be manually tracked (Mikkelsen *et al.*, 2004). Stagnant particles were deleted during the MATLAB routine before settling velocity was calculated, using the distance particles travel and the time between images. In addition, the bulk density of settling aggregates was estimated using an inverted Stoke's law method (Fox *et al.*, 2004; Curran *et al.*, 2004).

Large samples of bottom sediment collected from Douglas Channel in 2013-14 were used as the sediment component in wave tank experiments. Douglas Channel bottom sediment has been analyzed for disaggregated inorganic grain size (DIGS) using a Coulter Multisizer III electro-resistance particle counter, following methods described by Kranck and Milligan (1985) and Law *et al.* (2013). Organic components were removed from subsamples of bottom sediment using 35% hydrogen peroxide (H_2O_2). Remaining inorganic materials were resuspended in a 1% NaCl solution and disaggregated with a sapphire-tipped ultrasonic probe prior to analysis on the Coulter counter. Three aperture tubes (30, 200 and 400 µm) were used to measure particle size, and the results were merged in MATLAB to create continuous grain size spectra, covering a range of approximately 1 to 240 µm.

Water temperature (°C) and salinity (ppt) in the wave tank were measured with a handheld YSI system (model 30M). The concentration and distribution of suspended materials was monitored via water samples drawn from the tank (Figure 1) every 15-20 minutes at 5 and 145 cm depth at position A, 35 cm depth at position B (35 cm), and up to three depths at position D (5, 75 and 145). Sampling intensity was increased at position D during settling phases, and position A was not sampled during that time period. This sampling scheme produced approximately 70 water samples per experiment. Standard gravimetric methods were then used to vacuum-filter water samples onto pre-weighed Millipore 8.0 µm cellulose filters. These were dried (24 hours at 60°C), weighed, compared to pre-weights and divided by the volume of sample water filtered to determine the concentration (Law *et al.*, 2008). Pre-sediment water samples were also filtered to characterize the natural background concentration in the experiment water from the Bedford Basin, and processed for organic content. These filters (Whatman 25 mm glass fiber filters) were pre-washed, combusted at 550°C for 12 hours, and weighed prior to use.

3.0 RESULTS

Prior to the addition of sediment to the wave tank, the background concentration in experiment water was 0.5 - 3 $mg \cdot l^{-1}$, of which 50-80% was organic (Table 1). Following the addition of sediment to the tank, water samples showed that sediment was well-mixed within 60-100 minutes (Figures 2 and 3). Initial SPM at positions A, B and D was up to 60 $mg \cdot l^{-1}$ near the surface. With time and mixing, the concentration of material was gradually homogenized; within 60 minutes, SPM at the surface reduced to ~20 $mg \cdot l^{-1}$. Accordingly, SPM at 145 cm depth increased from background levels of ~2 $mg \cdot l^{-1}$ up to 5-20 $mg \cdot l^{-1}$ by the end of mixing (Figure 3). This confirmed that sediment was relatively evenly distributed throughout wave tank experiment water by the time oil (and dispersant where applicable) were added to the tank at 60 minutes. Bottom sediment sourced from the Douglas Channel area was generally fine and predominately composed of fine silts (~40%) and clays (~58%). Sand content was < 3%. Modal and median diameters were 2.6 and 5.0 µm, respectively. DIGS distributions presented here (Figure 4) are expressed by the log of volume concentration (ppm) plotted against the log of particle diameter (µm).

Results from each wave tank experiment were separated into three hour-long phases of interest for analysis. MVFC images and LISST data were analyzed at 5- and 15-minute increments (T = 0, 5, 15, 30, 45 and 60) throughout each phase to investigate the size distribution of suspended materials. Images collected by the MVFC during the addition of oil to the tank are shown in Figures 5 – 11; image collection was unsuccessful during WTE-16. Overall, merged particle size distributions were generally bimodal, with modes at approximately 10-20 and 120 µm (Figure 12 and 13). The maximum particle size identified at 35 cm depth during each experiment ranged from 400 - 600 µm, and occurred either following the addition of oil and dispersant, or during the settling phase. During chemically-dispersed experiments, the addition of oil and chemical dispersant to the tank regularly resulted in an influx of particles within minutes of the addition of oil and dispersant (Figure 12). Dispersed oil droplets covering a broad size range (50 µm - 1.0 mm) were found at 35 cm depth within 1 - 5 minutes of adding oil and dispersant, and typically appeared as spheres or elongated globules in MVFC images (Figures 5, 6, 7, 8 and 10). These particles represent chemically-dispersed oil droplets driven into the water column by waves. During non-chemically dispersed experiments, a limited population of droplets > 150 µm was noted within 5-15 minutes of oil being added (Figures 9 & 11). These large-diameter, physically-dispersed oil droplets were introduced to the water column through wave action. Excluding their occasional influence, post-oil particle size curves were very similar to pre-oil conditions in the absence of dispersant.

Depletion of smaller grain sizes (< 50 µm) at the MVFC/LISST location was typical over the course of settling phases, as fine particles were incorporated into an increasing population of larger particles (> 100 µm) that developed within 15-30 minutes of wave shut off. The progression toward larger particle sizes through floc growth was best defined during two non-chemically dispersed experiments (e.g. WTE-18 & 20), which showed a steady depletion of particles amongst smaller size classes (5-30 µm) (Figure 14). This reduction in the concentration of fine particles and subsequent growth in particles > 100 µm supports particle repackaging via flocculation. Similar dynamics occasionally occurred where dispersant was present (e.g. WTE-15 & 17), although in these cases the trend was not as well defined (Figure 14). Other chemically dispersed experiments (WTE-11 & 13) showed random, unorganized change at the fine end of particle size curves during settling phases, while particle growth at the coarse end was very minor or absent altogether (Figure 14).

The size range of dispersed oil droplets in suspension was estimated through subtraction of particle size spectra representing pre- and post-oil conditions (Figure 15). Particle size spectra derived from MVFC images were used for this exercise due to the notable change in the population of particles >100 µm in response to the dispersant. Where chemical dispersant was present, oil droplets were abundant and size distributions generally normal, with modes from 120-230 µm and maximum droplet sizes ranging from ~400-750 µm (Figure 15). In the absence of chemical dispersant, a limited number of oil droplets were forced into the water column by wave action. In these cases oil droplets were sized 100-550 µm (Figure 15).

The SVS-MVFC tracked settling particles that reached the bottom of the tank (145 cm). Size versus settling analysis was performed on images collected at this location at five minute intervals throughout the settling phase. Size versus settling relationships showed particles sized 30 - 330 µm settling at velocities ranging from 0.04 to 2.0 $mm \cdot s^{-1}$ (Figures 16 to 21). Data collection with the SVS-MVFC was unsuccessful during two experiments (WTE-11 & 15). In the presence of chemical dispersant, mean settling velocity was consistently lower (~0.20 $mm \cdot s^{-1}$) than those experiments where dispersant was not applied (~0.37 $mm \cdot s^{-1}$) (Table 3), regardless of particle density. Mean particle size observed during chemically dispersed experiments (91.4 µm) tended to be smaller than that observed during non-chemically dispersed experiments (106.5 µm). Effective particle density, described as the density of particles less that of seawater (1.020 $kg \cdot m^{-3}$), showed a wide range (7 to 735 $kg \cdot m^{-3}$) where particle density was notably higher under non-chemically dispersed conditions. In addition, the variation amongst settling velocity and density values was greater in non-chemically dispersed experiments. The highest mean particle density was encountered during non-chemically dispersed conditions (WTE-20-NCD); these particles also proved to be the fastest-settling of all experiments (Figure 21). The largest per-experiment mean particle size

(120.9 µm) also occurred in response to non-chemically dispersed conditions (WTE-16), and was associated with moderate settling velocities (0.37 $mm \cdot s^{-1}$) and particle densities (87.6 $kg \cdot m^{-3}$).

4.0 DISCUSSION

4.1 WARM WATER

Research described in this report provides unique transport parameters for predictive models designed to forecast the fate of diluted bitumen spilled in the marine environment. Warmer water (> 10°C) with low suspended sediment concentration (~15 mg L^{-1}) did not allow for OMA formation in the wave tank. OMA were not identifiable in images of suspended particles collected at two depths (35 and 145 cm). The absence of OMA was confirmed by microscope. The limited, two hour time scale for OMA formation could be a restrictive factor for OMA formation during wave tank experiments reported here. Work by Hill *et al.* (2002) suggests that formation times for stabilized OMA can be up to 24 hours, and that when OMA did form at lower sediment concentrations (~25 mg L^{-1}) the formation time was > 24 hours. In addition, formation was fastest with large oil droplets and high sediment concentration (> 200 mg L^{-1}). The duration of the settling phase during wave tank experiments, at the current testable sediment concentration (15 mg L^{-1}), was therefore likely not sufficient to facilitate the formation of OMA. Based on previous research using other oil products (Khelifa *et al.*, 2008b; Ajijolaiya *et al.*, 2006; Hill *et al.*, 2002), it is anticipated that OMA formation will be more efficient with a higher sediment concentration (e.g. 50 mg L^{-1}), as well as a longer period for sediment to interact with oil. Preliminary results from a 24 hour warm-water chemically dispersed wave tank experiment, where material was allowed to settle for 22 hours from a 50 mg L^{-1} sediment concentration, shows OMA formation – these data will be presented in subsequent reports. Further 24 hour experiments will continue to explore thresholds within this range to determine more accurately the mechanisms and characteristics of dilbit-derived OMA formation processes.

Merged particle size spectra derived from MVFC and LISST data showed that the application of chemical dispersant resulted in a greater concentration of larger diameter particles at 35 cm depth (Figure 22). This was demonstrated by a pulse of dispersed oil droplets immediately following the application of oil and dispersant. The concentration of droplets rapidly decreased at the MVFC/LISST location as they were diluted and distributed throughout the tank. Log-log plots of merged results show that particle size curves typically resumed pre-oil shapes within 15 to 30 minutes (Figure 22). While a large amount of oil entered the water column initially, the likelihood that larger oil droplets returned to the surface is high (Li *et al.*, 2009). A limited population of

discrete, smaller droplets (50 - 200 μm) were noted at 35 cm throughout the remainder of chemically dispersed experiments following the initial addition. When chemical dispersant was not applied (e.g. WTE-18, 20), any dispersion of oil was physically caused by breaking waves, and the addition of oil produced a contrastingly low concentration of oil droplets (Figure 11). Oil droplets that did occur were discrete and tended to be relatively small (< 200 μm) (Figures 9 and 11), although larger droplets (< 500 μm) appeared very sporadically at the sampling depth over the course of the second mixing phase due to wave forcing.

The presence of chemical dispersant produced two dominant responses during settling phases in the wave tank (Figure 23). At the MVFC/LISST location, these responses ranged from well-pronounced settling of particles sized < 30 μm (e.g. WTE-13, 15 & 17), to almost no change in the general particle population (e.g. WTE-11, 19) (Figure 13). Well-pronounced settling occurred during both WTE-13 and WTE-15, and both showed growth at the coarse end of grain size spectra, demonstrated by the appearance of larger (330-550 μm), non-spherical particles late in the settling phase (Figure 14). The timing of the appearance of these particles, preceded by the orderly, generally unbiased consumption of fines, suggests that they are products of flocculation (Kranck and Milligan, 1980). Prevailing flocculation processes in the presence of chemical dispersant conflicts with previously reported wave tank results (e.g. O'Laughlin *et al.*, 2016), which suggested that chemical dispersant may disrupt fine sediments' natural tendency to flocculate at low sediment concentration (e.g. 15 mg/L). However, this conflict follows the reported improvement in dispersant performance in warmer water (Li *et al.*, 2010; Sørensen *et al.*, 2013): oil is less viscous in warmer water, which enhances dispersant efficiency. As a result, it is possible that dispersant was consumed by interactions with oil and the impact on sediment was reduced, and accordingly the potential for flocculation increased.

Other chemically dispersed experiments reported here (e.g. WTE-11, 17 & 19) did not show particle growth comparable to that seen in WTE-13 & 15. It is possible this discrepancy was linked to the effectiveness of individual dispersant applications. Dispersant was manually applied to the oil slick via a hand-held pressure nozzle during wave tank experiments, and this process may have been adversely affected by atmospheric conditions such as wind. Particle size spectra derived from MVFC images characterizing the period immediately after dispersant applications were generally similar (Figure 22) and do not provide much insight. To more effectively investigate dispersant efficacy, entropy analysis of raw greyscale images was used to identify similarities in particle size distribution characteristics. Entropy analysis has previously been applied to evaluate dispersant efficacy (Li *et al.*, 2011), and was completed using a semi-automated MATLAB code (Mikkelsen *et al.*, 2007a). Entropy analysis was used here to compare the shape of particle size distributions derived from MVFC images

collected immediately following dispersant application, to determine the overall effectiveness of each dispersant application. Two general groups emerged from this analysis, with dimensionless entropy values (*E*) that are > or < 6 (Figure 24). One group (WTE-11, 17 & 19) (*E* > 6) showed broader particle size distributions with more rounded peaks, implying better size sorting than others (WTE-13 & 15, *E* < 6) that showed narrower, taller curves with sharper peaks (Figure 24). These results suggested that WTE-19 was the best sorted suspension following the addition of chemical dispersant, implying that this was the most effective dispersant application. This position is supported by calculations of dynamic dispersion effectiveness (DDE), which can determine the amount of oil (%) that is dispersed into the water column, at two points during each experiment (T=60 min & T=180 min) (Table 4). Dynamic dispersion effectiveness is expressed as

$$DDE(\%) = \frac{\bar{C}_{effluent}\, Q_{effluent}\, T + \bar{C}_{sample} V_{wt}}{\rho_{oil}\, V_{oil}}\ x\ 100,$$

where $\bar{C}_{effluent}$ is the time-averaged oil concentration in the effluent carried out of the wave tank (g·L^{-1}); $Q_{effluent}$ is the flow rate of the current (L·min^{-1}); V_{wt} is the total volume of water in the tank (27,000 L); T is the experiment duration (60 min); $\bar{C}_{sample}$ is the average concentration of oil remaining in the wave tank after T; ρ_{oil} is the density of the test oil (g·L^{-1}); and V_{oil} is the volume of oil used in each experiment (230 - 250 ml) (Li *et al.*, 2010). Results of this calculation showed that WTE-19 is the only experiment to experience increasing DDE over its duration. This suggests that this experiment may have formed the smallest oil droplets, which were capable of remaining in suspension from dispersion until the settling phase, and resulted in an increase in DDE over time (Li *et al.*, 2009). The success of this particular dispersant application is supported by wind conditions for the Bedford Basin (Table 5), which show notably lower wind conditions (a) over the course of this particular experiment, and (b) at the time dispersant was actually applied. Overall, this suggests that chemically dispersed experiments WTE-13 and WTE-15 showed particle growth at the coarse end of grain size curves late in the settling phase in response to less effective dispersant applications. Wind conditions were relatively high at the time of application in these cases (Table 5), which could have impacted the dispersant application and as a result compromised the total dispersant efficacy. This allowed for the natural tendency of flocculation to dominate particle dynamics during these wave tank experiments. Where dispersant application was most effective, e.g. not disrupted by wind, flocculation is restricted and particle growth through flocculation does not occur (e.g. WTE-19). The mechanisms for this restriction remain unclear. One possible explanation is the effect of chemical dispersant on sediment. Dispersants contain surfactants that orient at the oil-water interface to reduce

the interfacial surface tension and enable an oil slick to break-up into smaller droplets. It is possible that this could prevent sediment particles from adhering to one another to produce flocs. An alternative explanation may be a lack of fine particles (10 – 40 μm) with which to grow flocs. An abundance of small oil droplets entering the water column may accelerate the consumption of fine particles and limit flocculation; however this alternative implies OMA formation, and is not likely as no OMA were observed. Overall, these results suggest that when dispersant application is most effective, flocculation and subsequent settling of fine sediment flocs may be reduced. However, natural sediment flocculation can persist when dispersant application is less effective, such as in windy conditions, when dispersion may not be sufficient to promote the dominance of smaller oil droplets in the water column.

The size of suspended oil droplets was found to be smaller where chemical dispersant is present, compared with the limited number of non-chemically dispersed oil droplets that successfully penetrate the water column (Figure 15). Chemically dispersed conditions produced an abundance of suspended oil droplets, with modes ranging from 120-230 μm and droplet sizes from ~40 μm – 1 mm. Size distributions were unimodal. This range of droplet sizes is broader than in non-chemically dispersed conditions and includes a greater population of smaller droplets (<100 μm). During non-chemically dispersed experiments, low concentrations of oil droplets occurred at the sampling depth of 35 cm. These ranged in size from approximately 100 - 650 μm, and show size distributions with no clearly discernable mode. In general, these results support the notion that non-chemically dispersed dilbit resists sinking, at least on the short time scale tested here, and that chemically dispersed oil droplets tend to be smaller than physically (non-chemically) dispersed oil droplets.

Size versus settling results showed that mean settling velocity was consistently lower during chemically dispersed experiments (~0.20 $mm \cdot s^{-1}$) than those experiments where dispersant was not applied (~0.37 $mm \cdot s^{-1}$) (Table 3). A standard two-sample T-test shows that differences in settling velocity between chemically and non-chemically dispersed experiments is statistically significant (P = 0.006). Previous field studies of settling floc dynamics have described settling velocities on the order of 1.0 $mm \cdot s^{-1}$ (Hill *et al.*, 2000; Curran *et al.*, 2007); mean settling velocities measured during wave tank experiments reported here (0.1 – 0.5 $mm \cdot s^{-1}$) are slightly lower (Table 3). However it is important to note that the studies referenced measured the dynamics of high-concentration suspensions, ranging from tens to hundreds of milligrams per liter. Additionally, non-chemically dispersed experiments produced larger (107.8 μm) and denser (105.5 $kg \cdot m^{-3}$) particles compared with those produced by chemically dispersed conditions (91.7 μm, 81.7 $kg \cdot m^{-3}$) (Figures 16, 18 & 20), although these variances are not statistically significant (P = 0.093, 0.293).

The effective clearance rate (w_e) is designed to consider the overall rate of removal of particles from the water column, and for the purpose of this study, to evaluate change in the presence or absence of chemical dispersant. The effective, or bulk mean, clearance rate is the settling velocity necessary to explain the rate at which particles are removed from the water column through settling, under the assumption that the water column is well-mixed. This is expressed as

$$C(t) = C_0 e^{-(w_e/h)t},$$

where C(t) is the observed concentration ($g \cdot l^{-1}$) at time t (s), C_0 is the concentration ($g \cdot l^{-1}$) at time t=0, w_e is the effective clearance rate ($m \cdot s^{-1}$), and h is the SPM sample depth (m) (Curran *et al.,* 2004). Clearance rates reported here were developed from SPM values from water samples drawn from the wave tank at 5 cm depth at position D. Clearance rates on the order of 0.1 $mm \cdot s^{-1}$ have been reported for high concentrations of flocculated fine sediment in the marine environment (Curran *et al.,* 2004). By comparison, clearance rates reported here were low and ranged from <0.001 up to 0.08 $mm \cdot s^{-1}$. Mean values for chemically dispersed and non-chemically dispersed conditions (0.013 and 0.029 $mm \cdot s^{-1}$, respectively) showed that in this set of experiments, non-dispersed particles cleared the water column at a faster rate. It is likely that during non-chemically dispersed experiments, comparatively larger, denser, and therefore faster-settling particles developed in response to the absence of chemical dispersant. This lends support to the idea that the presence of chemical dispersant may impact natural flocculation processes, either by reducing the density of flocs, or by preventing floc growth altogether.

4.2 COMPARED WITH COLDER (<10°C) WATER

A previously published companion report (O'Laughlin *et al.*, 2016) described results from a series of colder water (<10°C), 15 $mg \cdot L^{-1}$ wave tank experiments. These experiments are suitable for direct comparison with warmer water (> 10°C) experiments described in this report. All experiments, parameters and testable conditions are summarized in Table 1. In both colder and warmer water, the application of chemical dispersant generated a rapid influx of chemically-dispersed oil droplets into the water column. Following this event, the concentration of suspended particles in the vicinity of the MVFC/LISST quickly dropped as oil droplets dispersed or resurfaced. In general, the results of wave tank experiments support the effectiveness of chemical dispersant in dispersing spilled dilbit, but do not suggest the formation of OMA, regardless of water temperature, at a mineral concentration of 15 $mg \cdot l^{-1}$.

The application of dispersant generally produced more fine particles (< 40 µm) in warmer water, compared with colder (Figure 25). This response may be attributed to the decreased viscosity of oil associated with higher water temperatures, and the associated improvement in chemical dispersant efficacy (Li *et al.*, 2010; Sørensen *et al.*, 2013). Experiments where chemical dispersant was not applied showed only minor increases in particle size in response to the addition of dilbit to the tank (Figure 25). This response was similar in both colder and warmer water experiments, suggesting that limited amounts of non-chemically dispersed oil entered the water column regardless of water temperature. This supports the notion that non-chemically dispersed dilbit is ineffective at penetrating the water column in the absence of chemical dispersant, even with the addition of mineral fines (Government of Canada, 2013). During settling phases, chemical dispersant use was associated with limited change to particle size spectra (Figure 14). Where change did occur, it was limited to occasional growth at the coarse end of particle size curves (e.g. WTE-3, 13), and settling in particles sized < 30 - 40 µm (e.g. WTE-10, 15) (Figure 14). In the absence of chemical dispersant, both colder and warmer water experiments showed a tendency toward particle growth through flocculation, and showed comparatively greater amounts of settling in material < 40 µm (e.g. WTE-18, 20) (Figure 14). As mentioned, this may indicate a link between the use of chemical dispersant and disruption to the natural tendency of fine sediment to flocculate and settle.

MVFC imagery at 35 cm depth during WTE-15 showed particles that are unique in appearance compared with all other experiments (Figure 26). As particle size peaked ~30 minutes into the settling phase, a population of elongated, string-like particles emerged. A number of these particles, composed of a mixture of irregular shapes, long stringy particles and perfect spheres, adopted a comet-like appearance with a broad head and narrower tail. They visually appeared to be of relatively low density and appeared to include a large proportion of organic-type particles. Such elongated droplets are common with heavy crude oils, as small oil particles are shed from larger droplets leaving a tracer effect and producing a comet-like structure as they sink into the water column. Similarly, the settling motion of large flocs can create a wake that pulls in and incorporates other small particles to produce a drawn-out tail. Water quality data from the Bedford Basin, which was the source of wave tank experiment water, showed elevated particulate organic carbon (POC) and chlorophyll levels during the week of chemically dispersed experiment WTE-15 (Figure 27). High water temperature during the autumn season coupled with these elevated values suggests that an active algae bloom in the Basin was the likely cause of high levels of organic content in wave tank experiment water. As a result, organic material in basin water pumped into the wave tank (Table 1) was not effectively excluded by filtering. The role of organic content in the flocculation process is related primarily to sticky, bacteria-laden coatings, which increase the adherence of inorganic particles and

facilitates floc formation (Eisma, 1986; Kranck, 1973). High organic content suspensions produce large, low-density flocs that settle slowly, and in this case are likely to interact with dispersed oil droplets to produce elongated, stringy particles, which include both sediment flocs and oil droplets. Unfortunately, the SVS-MVFC camera did not capture images of these particles. Non-chemically dispersed experiments (e.g. WTE-18 and 20) completed in subsequent weeks showed similarly elevated levels of organics in wave tank experiment water pumped in from Bedford Basin, but did not develop similar string-like particles. This could be explained by the absence of chemical dispersant and the resulting low concentration of oil in the water column in these cases.

Size versus settling analysis showed notable differences in the size and settling relationships of particles in colder and warmer water conditions (Figure 28). Mean values for all colder water experiments show that these produced generally smaller particles of higher density (86.52 µm, 110.5 $kg \cdot m^{-3}$) compared with warmer water conditions (99.76 µm, 93.73 $kg \cdot m^{-3}$). The difference in particle size between cold and warm water experiments was statistically significant ($P = 0.043$). Larger particles produced during warm water conditions settled faster (0.285 $mm \cdot s^{-1}$) than smaller, denser particles occurring during colder water conditions (0.164 $mm \cdot s^{-1}$). Variability in settling velocity was statistically significant ($P = 0.022$), whereas that of effective particle density was not ($P = 0.540$). Effective particle density was generally higher in colder water experiments, although this variability was not statistically significant ($P = 0.540$). This may be associated with changing fractal geometry of flocs, in response to the behaviour of organics in colder versus warmer water (Meakin, 1988). Increasing amounts of organic material within the interstitial spaces of flocs can grow particle density and cause faster settling. Size settling and effective density relationships allow for inferences on the fractal dimensions of flocs (e.g. Dyer and Manning, 1999). In data considered here, changes in the fractal dimensions of flocs did not appear to correlate with the concentration of organics in the water. In warmer water, particles produced in response to the presence of chemical dispersant were notably less dense (81.96 $kg \cdot m^{-3}$) than those produced in the absence of chemical dispersant (105.5 $kg \cdot m^{-3}$). These were less dense than in cold water conditions, which gave similar density results for particles produced with (110.16 $kg \cdot m^{-3}$) and without chemical dispersant (110.68 $kg \cdot m^{-3}$). Grouping results into dispersed and non-dispersed categories showed similar trends, where particles in non-chemically dispersed conditions are larger, denser and settle faster.

Dispersed oil droplets were generally larger in colder water conditions (Figure 29), a result that supports the improved effectiveness of chemical dispersant in warmer water. Smaller oil droplets have lower buoyancy, are more likely to remain in the water column to be biodegraded and are less likely to resurface (Li *et al.*, 2011). Non-chemically dispersed conditions produced substantially lower concentrations of oil

droplets in the water column, although the size range of these droplets was similar to that of chemically dispersed conditions. Particle size curves in these cases were unorganized, showed gaps in size distributions and lacked well-defined modes. This was generally true for both colder and warmer water conditions.

Clearance rates for chemically dispersed and non-chemically dispersed experiments showed similar variability, on the order of 0.01 – 0.1 $mm \cdot s^{-1}$; however mean values were higher for non-dispersed experiments (0.04 $mm \cdot s^{-1}$) compared with chemically-dispersed (0.03 $mm \cdot s^{-1}$). In terms of water temperature, particles generally cleared the water column faster in colder water (< 10°C) conditions (0.04 & 0.05 $mm \cdot s^{-1}$, for chemically dispersed and non-chemically dispersed colder water groupings, respectively) compared with warmer water (> 10°C) conditions (0.01 & 0.03 $mm \cdot s^{-1}$, for chemically dispersed and non-chemically dispersed warm water groupings, respectively). These results support the improved effectiveness of chemical dispersant at warmer water temperatures, but again do not suggest *in situ* OMA formation.

5.0 CONCLUSION

Wave tank experiments operating at 15 $mg \cdot l^{-1}$ in warmer water (> 10°C) were unsuccessful at *in situ* formation of OMA. The absence of OMA was confirmed via microscopy. This was likely a result of factors including the short time scale (e.g. two hours) provided for oil-sediment interaction during wave tank experiments, and the relatively low concentration of suspended sediment. Further experiments will be carried out at 50 $mg \cdot l^{-1}$ will consist of longer settling periods (>20 hrs) and are more likely to result in OMA formation. The results of this study confirm that the presence of chemical dispersant facilitates higher concentrations of oil droplets entering the water column compared with conditions that are limited to physical dispersion. In the absence of chemical dispersant, particles produced were larger and denser, and settled almost two times faster than chemically dispersed particles. These results were similar for both colder (< 10°C) and warmer water conditions. Additionally, results suggest a reduced potential for flocculation of fine sediment in the presence of chemical dispersant, at low suspended sediment concentration. Overall, the number of oil droplets that entered the water column during non-chemically dispersed conditions was limited. In general, these results support the effectiveness of chemical dispersant on diluted bitumen, but do not suggest the formation of OMA under the tested conditions.

ACKNOWLEDGEMENTS

This research was supported by the Ocean Protection Plan (OPP), formerly World Class Tanker Safety (WCTS) program, from Fisheries and Oceans Canada. Special thanks are

owed to COOGER staff for wave tank operations and preparing samples for laboratory experiments, and to Particle Dynamics Lab staff for grain size and image processing.

REFERENCES

Ajijolaiya, L.O., Hill, P.S., Khelifa, A., Islam, R.M., Lee, K. 2006. Laboratory investigation of the effects of mineral size and concentration on the formation of oil–mineral aggregates. Marine Pollution Bulletin 52: 920–927. http://dx.doi.org/10.1016/j.marpolbul.2005.12.006

Curran, K.J., Hill, P.S., Milligan, T.G., Mikkelsen, O.A., Law, B.A., Durrieu de Madron, X., Bourrin, F. 2007. Settling velocity, effective density, and mass composition of suspended sediment in a coastal bottom boundary layer, Gulf of Lions, France. Continental Shelf Research 27: 1408–1421. http://dx.doi.org/10.1016/j.csr.2007.01.014

Curran, K.J., Hill, P.S., Milligan, T.G. 2002. Fine-grained suspended sediment dynamics in the Eel river flood plume. Continental Shelf Research 22: 2537-2550.

Curran, K.J., Hill, P.S., Schnell, T.M., Milligan, T.G., Piper, D.J.W. 2004. Inferring the mass fraction of floc deposited mud: application to fine-grained turbidites. Sedimentology 51: 927–944.

Dyer, K.R. and Manning, A.J. 1999. Observation of the size, settling velocity and effective density of flocs, and their fractal dimensions. Journal of Sea Research 41: 87–95. http://dx.doi.org/10.1016/S1385-1101(98)00036-7

Eisma, D. 1986. Flocculation and de-flocculation of suspended matter in estuaries. Netherlands Journal of Sea Research 20(2-3): 183–199.

Fox, J.M., Hill, P.S., Milligan, T.G., Boldrin, A. 2004. Flocculation and sedimentation on the Po River Delta. Marine Geology 203: 95–107. http://dx.doi.org/10.1016/S0025-3227(03)00332-3

Gong, Y., Zhao, X., Cai, Z., O'Reilly, S.E., Hao, X., Zhao, D. 2014. A review of oil, dispersed oil and sediment interactions in the aquatic environment: Influence on the fate, transport and remediation of oil spills. Marine Pollution Bulletin 79: 16–33. http://dx.doi.org/10.1016/j.marpolbul.2013.12.024

Government of Canada. 2013. Federal Government Technical Report: Properties, composition and marine spill behaviour, fate and transport of two diluted bitumen products from the Canadian oil sands. pp. 1–85, ISBN 978-1-100-23004-7 Cat. No.: En84-96/2013E-PDF.

Hill, P.S., Khelifa, A., Lee, K. 2002. Time scale for oil droplet stabilization by mineral particles in turbulent suspensions. Spill Science & Technology Bulletin 8 (1): 73–81. http://dx.doi.org/10.1016/S1353-2561(03)00008-2

Khelifa, A., Chun, M., Eubank, J.L.E., Brown, C.E. 2008a. Physical properties of oil- SPM aggregates: experiments with the NIST standard reference material 1941b, In: Proceedings of the 31st AMOP technical seminar on environmental contamination and response, Environment Canada, Ottawa, ON: Vol. 1, pp. 35–51.

Khelifa, A., Fingas, M., Brown, C. 2008b. Effects of Dispersants on Oil-SPM Aggregation and Fate in US Coastal Waters: Final Report Submitted to The Coastal Response Research Center, March 2008, pp. 57.

Khelifa, A., Fieldhouse, B., Wang, Z., Yang, M., Landriault, M., Fingas, C.E., Brown, C.E., Gamble, L. 2007. A Laboratory Study on formation of Oil-SPM aggregates using the NIST standard reference material 1941b, In: Proceeding of the Thirtieth Arctic and marine Oil Spill Program Technical Seminar, Environment Canada, Ottawa, ON: pp. 35–48.

Khelifa, A., Hill, P.S., Lee, K. 2005. Assessment of minimum sediment concentration for OMA formation using a Monte Carlo model, In: Al-Azab, M., El-Shorbagy, W., Al-Ghais, S. (Eds.), Oil Pollution and its Environmental Impact in the Arabian Gulf Region. Elsevier, pp. 93–104. http://dx.doi.org/10.1016/S1571-9197(05)80031-X

Khelifa, A., Stoffyn-Egli, P., Hill, P.S., Lee, K. 2002. Characteristics of oil droplets stabilized by mineral particles: effects of oil type and temperature. Spill Science & Technology Bulletin 8 (1): 19-30.

King, T.L., Robinson, B., Boufadel, M., Lee, K. 2015. Flume tank studies to elucidate the fate and behavior of diluted bitumen spilled at sea. Mar. Pollut. Bull. (2014), http://dx.doi.org/10.1016/j.marpolbul.2014.04.042

King, T., Robinson, B., Ryan, S., Lu, Y., Zhou, Q., Ju, L., Li, J., Sun, P., Lee, K. 2015. Fate of Chinese and Canadian Oils Treated with Dispersants in a Wave Tank. Proceedings of the Thirty-Eighth AMOP Technical Seminar on Environmental Contamination and Response, Environment Canada, Ottawa, ON, 798-811.

Kranck, K. 1973. Flocculation of suspended Sediment in the Sea. Nature 246: 348-350. http://dx.doi.org/10.1038/246348a0

Kranck, K. 1980. Experiments on the significance of flocculation in the settling of fine-grained sediment in still water. Can. J. Earth Sci.17: 1517–1526. http://dx.doi.org/10.1139/e80-159

Kranck, K., Milligan, T.G. 1992. Characteristics of suspended particles at an 11 hour anchor station in San Francisco Bay, California. Journal of Geophysical Research 97 (C7): 11,373–11,382.

Kranck, K., Milligan, T.G. 1985. Origin of Grain Size Spectra of Suspension Deposited Sediment. Geo-Marine Letters 5: 61-66.

Law, B. A., Hill, P. S., Milligan, T. G., Curran, K. J., Wiberg, P. L., & Wheatcroft, R. A. 2008. Size sorting of fine-grained sediments during erosion: results from the western Gulf of Lions. Continental Shelf Research, 28(15), 1935-1946. http://dx.doi.org/10.1016/j.csr.2007.11.006

Law, B.L., Milligan, T.G., Hill, P.S., Newgard, J., Wheatcroft, R.A., Wiberg, P.L. 2013. Flocculation on a muddy intertidal flat in Willapa Bay, Washington, Part I: A regional survey of the grain size of surficial sediments. Continental Shelf Research 60 (S): 136-144. http://dx.doi.org/10.1016/j.csr.2012.06.007

Lee, K., Bugden, J., Cobanli, S., King, T., McIntyre, C., Robinson, B., Ryan, S., Wohlgeschaffen, G. 2012. UV-Epifluorescence Microscopy Analysis of Sediments Recovered from the Kalamazoo River. US EPA Kalamazoo Administrative Record. Document, 1277.

Lee, K., Li, Z., King, T., Kepkay, P., Boufadel, M.C., Venosa, A.D., Mullin, J.V. 2008. Effects of chemical dispersants and mineral fines on partitioning of petroleum hydrocarbons in natural seawater. In: International Oil Spill Conference 2008, No. 1: 633–638.

Lee, K., Stoffyn-Egli, P., Tremblay, G.H., Owens, E.H., Sergy, G.A., Guénette, C.C., Prince, R.C. 2003. Oil–Mineral Aggregate Formation on Oiled Beaches: Natural Attenuation and Sediment Relocation. Spill Science & Technology Bulletin, Vol. 8, (3): 285–296. http://dx.doi.org/10.1016/S1353-2561(03)00042-2

Li, Z., Kepkay, P., Lee, K., King, T., Boufadel, M.C., Venosa, A.D. 2007. Effects of chemical dispersants and mineral fines on crude oil dispersion in a wave tank under breaking waves. Marine Pollution Bulletin 54: 983–993. http://dx.doi.org/10.1016/j.marpolbul.2007.02.012

Li, Z., Lee, K., King, T., Boufadel, M.C., Venosa, A.D. 2009. Assessment of chemical dispersant effectiveness in a wave tank under regular non-breaking and breaking wave conditions. Marine Pollution Bulletin 56: 903–912. http://dx.doi.org/ doi:10.1016/j.marpolbul.2008.01.031

Li, Z., Lee, K., King, T., Boufadel. M.C., Venosa, A.D. 2010. Effects of temperature and wave conditions on chemical dispersion efficacy of heavy fuel oil in an experimental flow-through wave tank. Marine Pollution Bulletin 60: 1550-1559.

Li, Z., Lee, K., King, T., Niu, H., Boufadel, M.C., Venosa, A.D. 2011. Application of entropy analysis of *in situ* droplet-size spectra in evaluation of chemical dispersion efficacy. Marine Pollution Bulletin 62: 2129-2136. http://dx.doi.org/10.1016/j.marpolbul.2011.07.012

Lindstrom, J.E., Braddock, J.F. 2002. Biodegradation of petroleum hydrocarbons at low temperature in the presence of the dispersant Corexit 9500. Marine Pollution Bulletin 44: 739–747. http://dx.doi.org/10.1016/S0025-326X(02)00050-4

Manning, A. J., & Dyer, K. R. 2002. A comparison of floc properties observed during neap and spring tidal conditions. Proceedings in Marine Science 5: 233-250. http://dx.doi.org/10.1016/S1568-2692(02)80019-5

McCave, I. N. 1984. Size spectra and aggregation of suspended particles in the deep ocean. Deep Sea Research Part A. Oceanographic Research Papers 31(4): 329-352. http://dx.doi.org/10.1016/0198-0149(84)90088-8

Meakin, P. 1991. Fractal aggregates in Geophysics. Reviews of Geophysics 29(3): 317-354. http://dx.doi.org/10.1029/91RG00688

Mikkelsen, O.A., Curran, K.J., Hill, P.S., Milligan, T.G. 2007. Entropy analysis of in situ particle size spectra. Estuarine Coastal and Shelf Science 72: 615-625. http://dx.doi.org/10.1016/j.ecss.2006.11.027

Mikkelsen, O.A., Milligan, T.G., Hill, P.S., Chant, R.J., Jago, C.F., Jones, S.E., Krivtsov, V., Mitchelson-Jacob, G. 2007. The influence of schlieren on in situ optical measurements used for particle characterization. Limnology and Oceanography Methods 6 (3): 133-143. http://dx.doi.org/10.4319/lom.2008.6.133

Mikkelsen, O.A., Milligan, T.G., Hill, P.S., Moffat, D. 2004. INSSECT—an instrumented platform for investigating floc properties close to the seabed. Limnology and Oceanography Methods 2: 226-236.

Milligan, T. G., Hill, P. S., & Law, B. A. 2007. Flocculation and the loss of sediment from the Po River plume. Continental Shelf Research, 27(3), 309-321. http://dx.doi.org/10.1016/j.csr.2006.11.008

Milligan, T. G., & Law, B. A. 2005. The effect of marine aquaculture on fine sediment dynamics in coastal inlets. In: Environmental Effects of Marine Finfish Aquaculture (239-251). Springer Berlin Heidelberg. http://dx.doi.org/10.1007/b136013

Niu, H., Lee, K. (2013). Study of the dispersion/settling of oil-mineral-aggregates using particle tracking model and assessment of their potential risks. Int. J. Environment and Pollution (52): 32–51. http://dx.doi.org/10.1504/IJEP.2013.056356

Niu, H., Li, Z., K., Lee, K., Kepkay, P., Mullin, J.V. 2011. Modelling the Transport of oil-mineral aggregates (OMAs) in the Marine Environment and Assessment of Their Potential Risks. Environmental Modelling and Assessment 16 (1): 61-75. http://dx.doi.org/ 10.1007/s10666-010-9228-0

O'Laughlin, C., Law, B.A., Zions, V.S., King, T.L., Robinson, B., Wu, Y. 2016. The dynamics of diluted bitumen derived oil-mineral aggregates, Part I. Can. Tech. Rep. Fish. Aquat. Sci. No. 3157.

Owens, E.H. 1999. The interaction of fine particles with stranded oil. Pure Applied Chemistry 71: 83-93.

Page, C.A., Bonner, J.S., Sumner, P.L., McDonald, T.J., Autenrieth, R.L., Fuller, C.B. 2000. Behaviour of a chemically dispersed oil and a whole oil on a nearshore environment. Wat. Res. 34 (9): 2507-2516. http://dx.doi.org/10.1016/S0043-1354(99)00398-X

Schneider, C.A., Rasband, W.S., Eliceiri, K.W. 2012. NIH Image to ImageJ: 25 years of image analysis. Nature Methods 9: 671-675.

Sørensen, L., Melbye, A.G., Booth, A.M. 2014. Oil droplet interaction with suspended sediment in the seawater column: Influence of physical parameters and chemical dispersants. Marine Pollution Bulletin 78: 146-152. http://dx.doi.org/10.1016/j.marpolbul.2013.10.049

Sternberg, R.W., Berhane, I., Ogston, A.S. 1999. Measurement of size and settling velocity of suspended aggregates on the northern California continental shelf. Marine Geology 154: 43-53. http://dx.doi.org/10.1016/S0025-3227(98)00102-9

Sun, J., Khelifa, A., Zhao, C., Zhao, D., Wang, Z. 2014. Laboratory investigation of oil–suspended particulate matter aggregation under different mixing conditions. Science of the Total Environment 473–474: 742–749. http://dx.doi.org/10.1016/j.scitotenv.2013.12.078

Sun, J., Zhao, D., Zhao, C., Liu, F., Zheng, X. 2013. Investigation of the kinetics of oil–suspended particulate matter aggregation. Marine Pollution Bulletin 76: 250–257. http://dx.doi.org/10.1016/j.marpolbul.2013.08.030

Venosa, A.D., Holder, E.L., 2007. Biodegradability of dispersed crude oil at two different temperatures. Marine Pollution Bulletin 54: 545–553. http://dx.doi.org/10.1016/j.marpolbul.2008.01.031

Van Der Lee, W.T.B. 2000. Temporal variation of floc size and settling velocity in the Dollard estuary. Continental Shelf Research 20 (12-13): 1495-1511.

Wang, W., Zheng, Y., Li, Z., Lee, K. (2011). PIV investigation of oil- mineral interaction for an oil spill application. Chemical Engineering Journal 170 (1): 241-249. http://dx.doi.org/10.1016/j.cej.2011.03.062

Wu, Y., C.G. Hannah, B. Law, T. King, and B. Robinson. 2016. An Estimate of the Sinking Rate of Spilled Diluted Bitumen in Sediment Laden Coastal Waters. Proceedings of the Thirty-ninth AMOP Technical Seminar, Environment and Climate Change Canada, Ottawa, ON, pp. 331-347, 2016.

Zhang, H., Khatibi, M., Zheng, Y., Lee, K., Li, Z., Mullin, J.V. 2010. Investigation of OMA formation and the effect of minerals. Marine Pollution Bulletin 60: 1433–1441. http://dx.doi.org/10.1016/j.marpolbul.2010.05.014

Zhao, L., Boufadel, M.C., Geng, X., Lee, K., King, T., Robinson, B., Fitzpatrick, F. 2016. A-DROP: A predictive model for the formation of oil particle aggregates (OPAs). Marine Pollution Bulletin 106 (1-2): 245-259. http://dx.doi.org/10.1016/j.marpolbul.2016.02.057

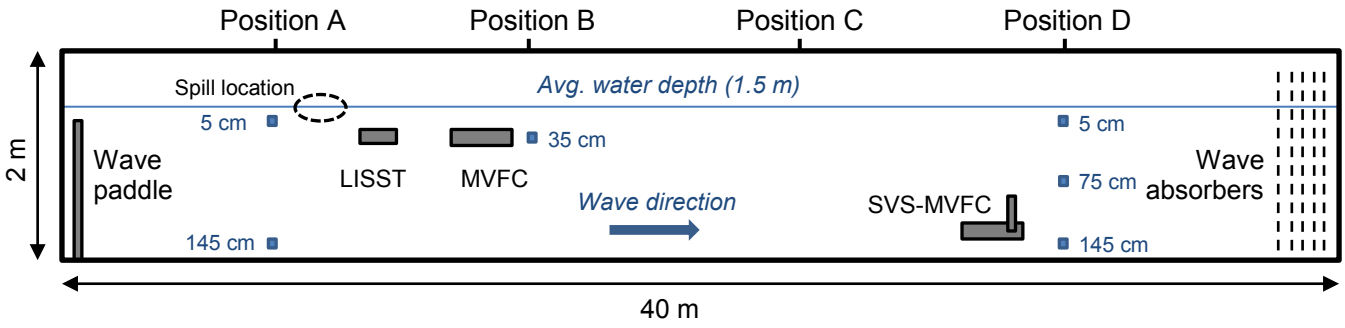

Figure 1: Wave tank schematic

The wave tank is 40 meters long and operates at a water depth of 1.5 meters. The locations of instruments and sampling stations are shown, along with the spill location where oil is added.

Experiment ID	Temp. (°C)	Salinity (ppt)	Background water		Sediment		Oil	
			SPM (mg/L)	Organic (%)	Station	Amount (g)	Type	Amount (g)
WTE-3-CD	4.0	28.5	1.76	58.0	DC-09	841.0	AWB	215.4
WTE-4-NCD	6.0	29.7	0.96	83.0	DC-05	1521.0	CLB	245.3
WTE-5-CD	9.0	30	1.64	58.0	DC-09	840.1	AWB	241.7
WTE-7-NCD	7.5	30.3	1.00	70.0	DC-09	841.7	AWB	261.4
WTE-8-NCD	10.2	29.6	1.84	66.0	DC-09	841.7	AWB	236.5
WTE-9-CD	10.2	30.3	2.24	54.0	DC-05	1526.4	CLB	245.4
WTE-10-CD	9.6	30.4	2.46	63.0	DC-09	840.1	AWB	249.7
WTE-11-CD	12.9	30.2	1.82	42.9	DC-26	1528.0	CLB	235.7
WTE-12-NCD	11.5	29.1	2.41	57.0	DC-05	1518.9	CLB	238.3
WTE-13-CD	13.1	29.6	1.25	49.2	DC-26	1523.3	CLB	252.2
WTE-15-CD	13.8	30.2	1.00	65.5	DC-26	1387.0	AWB	223.1
WTE-16-NCD	14.2	28.1	1.73	40.3	DC-26	1387.0	AWB	223.7
WTE-17-CD	12.1	30.7	1.08	41.8	DC-26	1396.0	AWB	238.8
WTE-18-NCD	13.2	31.1	0.57	70.0	DC-26	1390.0	AWB	229.9
WTE-19-CD	14.0	30.8	1.91	34.7	DC-26	1388.0	AWB	245.4
WTE-20-NCD	13.2	31.3	0.69	69.5	DC-26	1389.0	AWB	227.1

Table 1: Low sediment concentration (15 mg·l^{-1}) wave tank experiments

Experimental conditions from sixteen low concentration (15 mg·l^{-1}) wave tank experiments, including water temperature and salinity and the type and quantity of sediment and oil used. Sediment was sourced from three stations along Douglas Channel (British Columbia, Canada); station names describe the distance from Kitimat in nautical miles. Access Western Blend (AWB) and Cold Lake Blend (CLB) dilbits were used, in chemically dispersed (CD) and non-chemically dispersed (NCD) conditions (indicated by experiment ID). Results from warmer water (>10°C), low concentration (15 mg·l^{-1}) wave tank experiments discussed in this report are highlighted.

Dilbit product	% Weathered	Viscosity (centistokes)		Density (g/mL)	
		15°C	40°C	15°C	40°C
Cold Lake Blend (Winter Blend)	6.20%	1293.4	211.7	0.951	0.934
Access Western Blend (Winter Blend)	7.00%	1402.0	227.6	0.948	0.931

Table 2: Physical properties of oils used in this study.

Physical properties, including viscosity (centistokes) and density (g/mL) at 15 and 40°C, as well as weathering (%), for the two types of dilbit product used in this study.

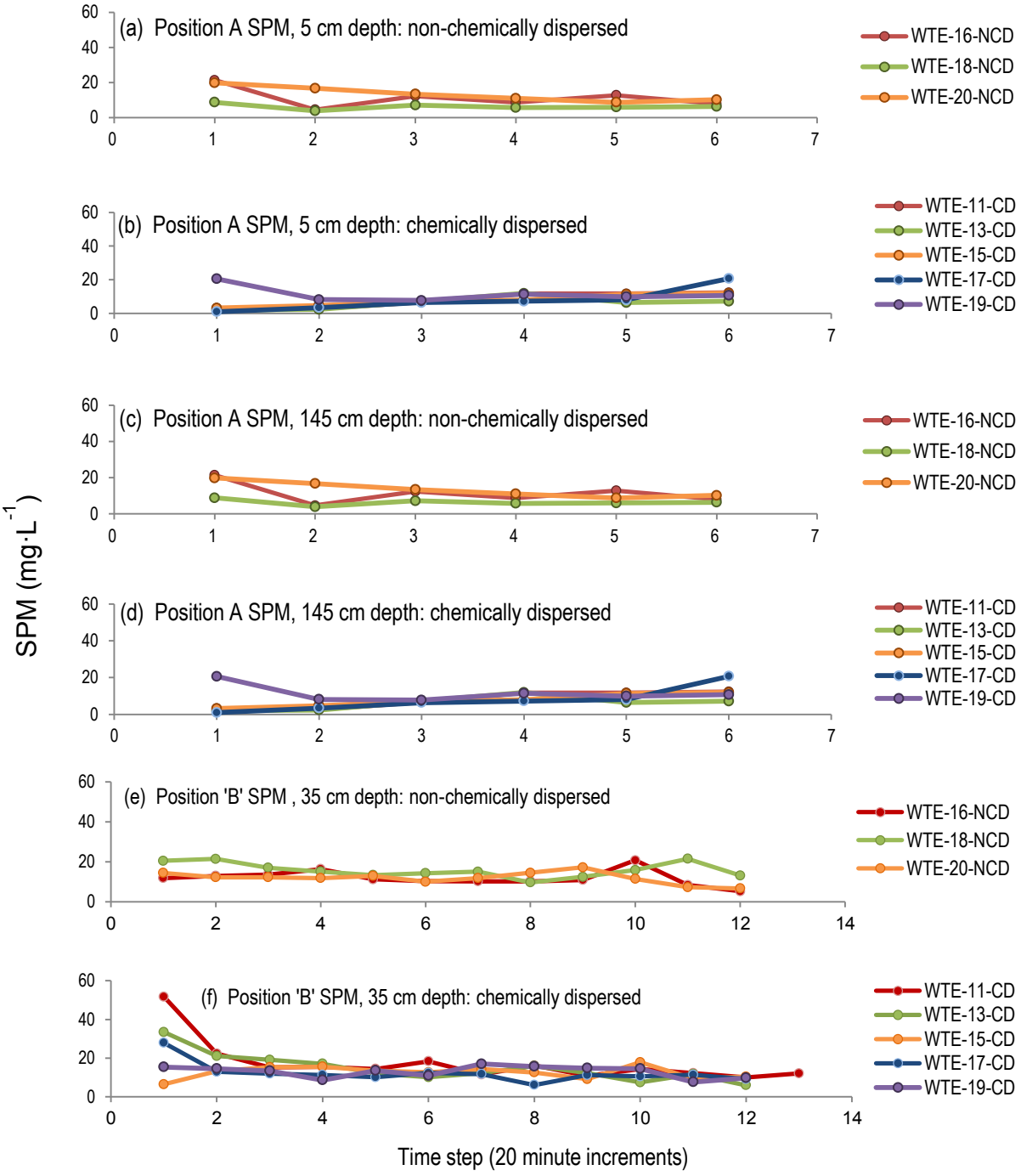

Figure 2: Suspended particulate matter (SPM), positions A and B

Suspended particulate matter (SPM) concentration at positions A (5 and 145 cm depth) and B (35 cm depth), derived from filtered water samples and grouped by the presence or absence of chemical dispersant. SPM concentration stabilizes rapidly following the addition of sediment, and was stable at 15-20 $mg \cdot l^{-1}$ for the duration of experiments. Oil and dispersant (where applicable) were added at T = 4.

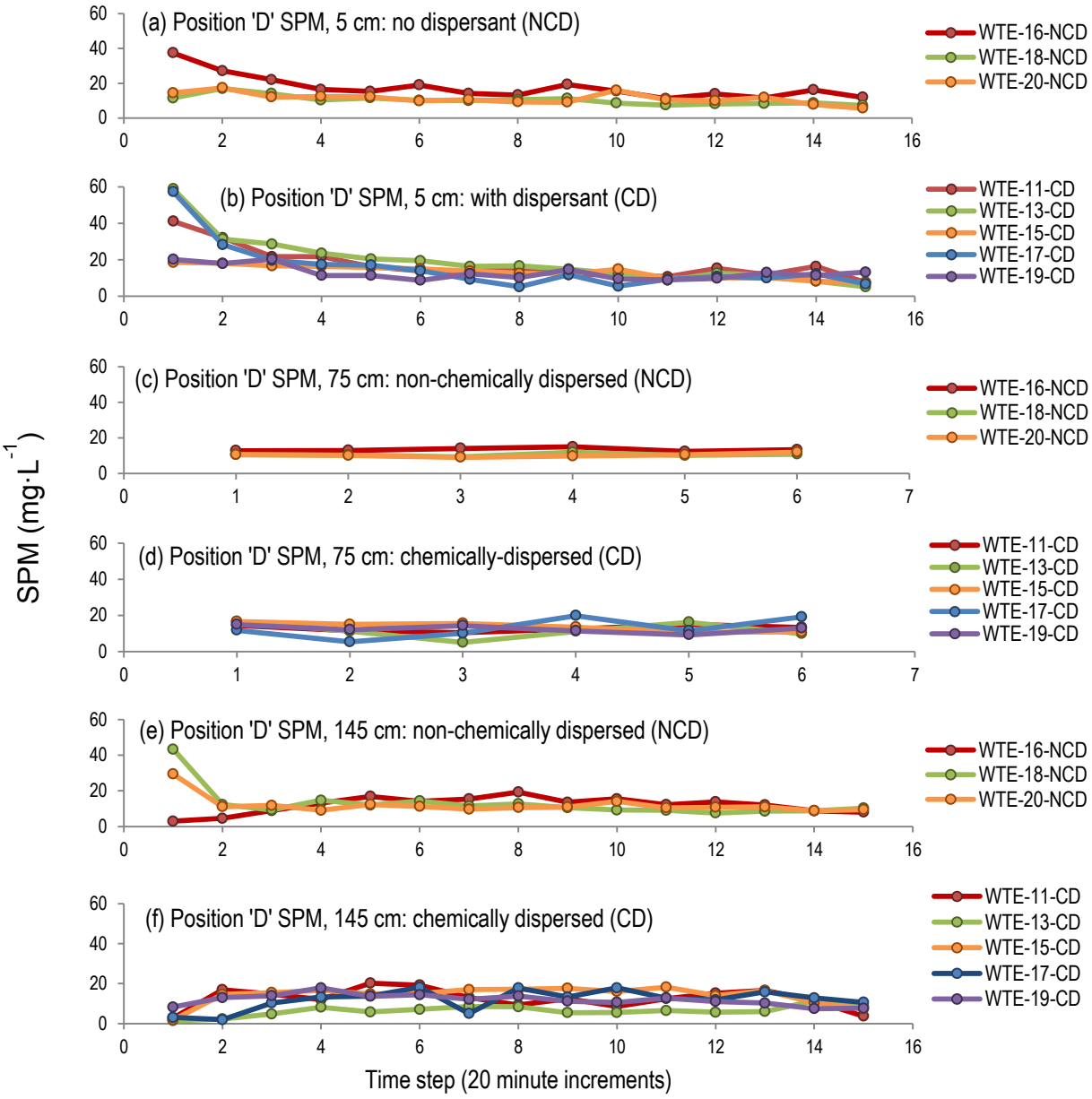

Figure 3: Suspended particulate matter (SPM), position C

Suspended particulate matter (SPM) concentration at position C (5, 75 and 145 cm), derived from filtered water samples and grouped by the presence or absence of chemical dispersant. Similar responses occurred in both chemically dispersed (CD) and non-chemically dispersed (NCD) experiments.

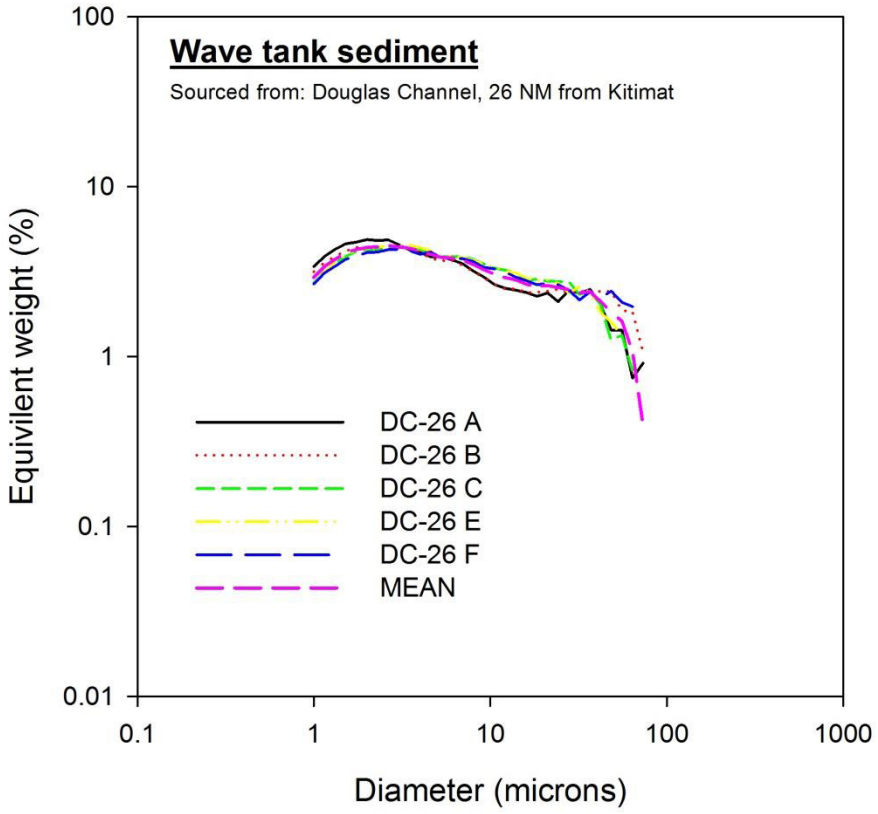

Figure 4: Disaggregated inorganic grain size (DIGS) spectra, Douglas Channel sediment

Bottom sediment collected from Douglas Channel in 2014 was used as the sediment component in wave tank experiments. Disaggregated inorganic grain size (DIGS) results, shown here, are expressed as the log of the volume concentration (ppm) versus the log of particle diameter (μm).

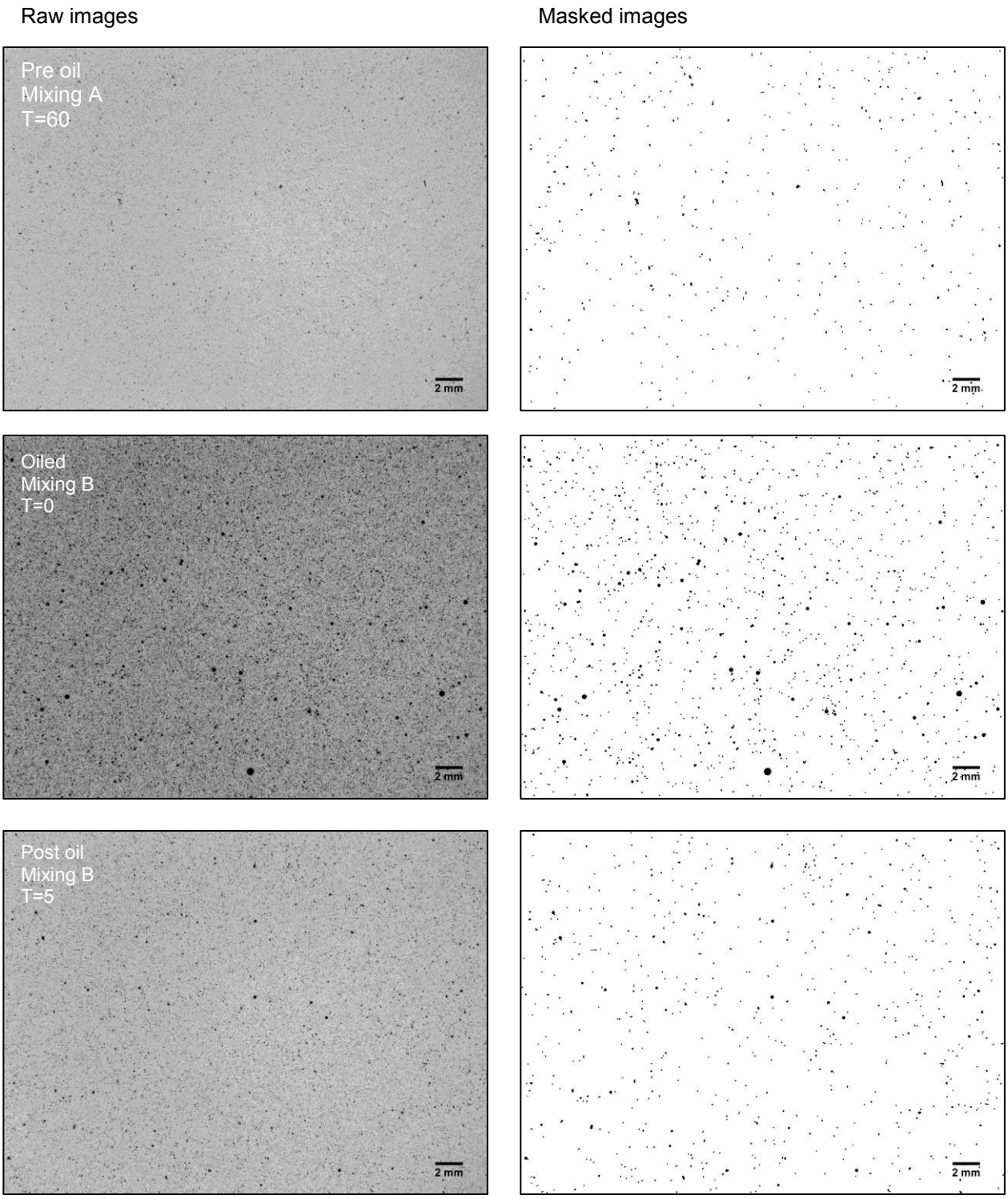

Figure 5: Raw and masked MVFC images, WTE-11-CD

WTE-11-CD raw (left) and masked (right) MVFC images, for pre-oil (Mixing A, T = 60), oiled (Mixing B, T = 0) and post-oil conditions (mixing B, T = 5).

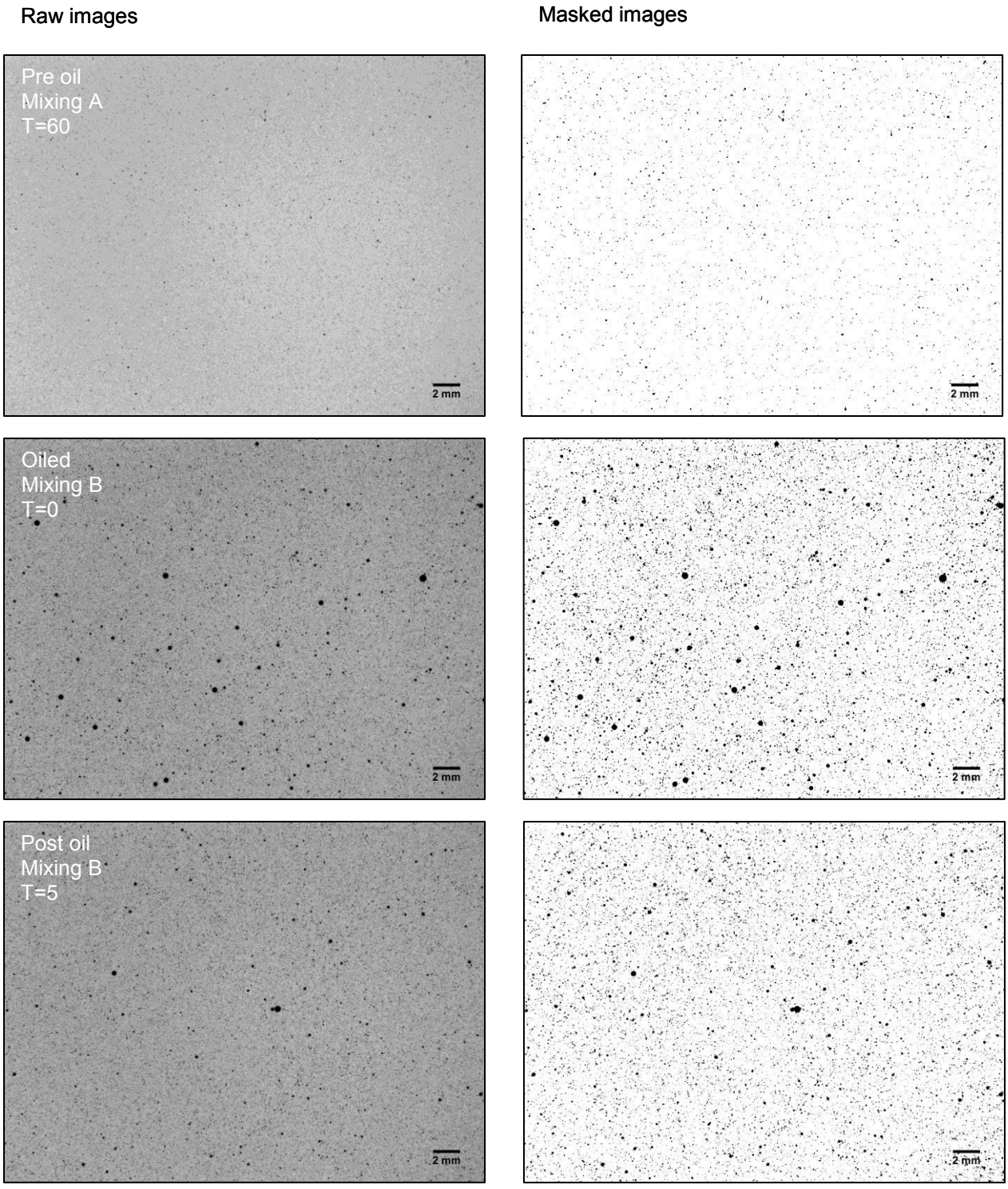

Figure 6: Raw and masked MVFC images, WTE-13-CD

WTE-13-CD raw (left) and masked (right) MVFC images, for pre-oil (Mixing A, T = 60), oiled (Mixing B, T = 0) and post-oil conditions (mixing B, T = 5).

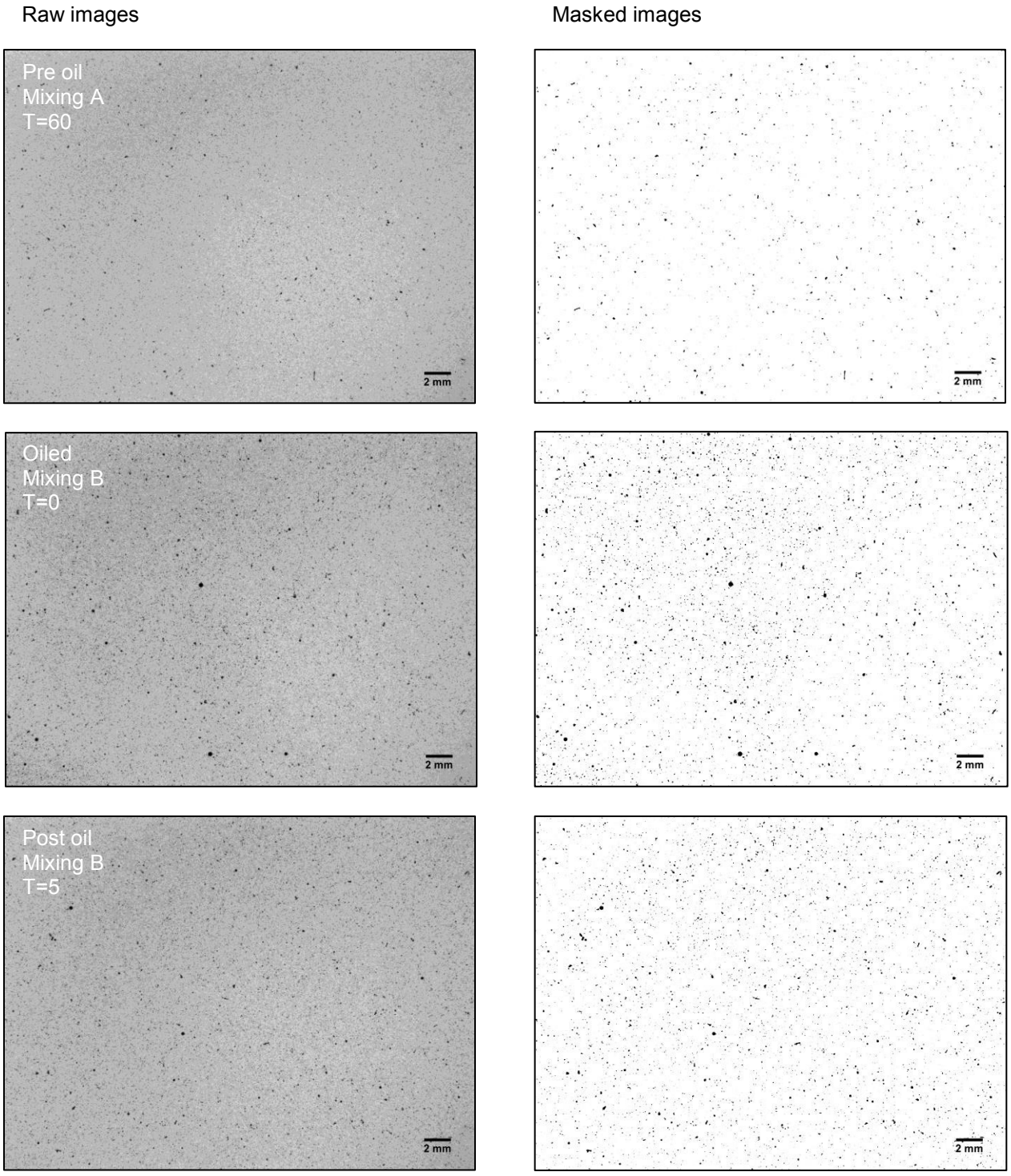

Figure 7: Raw and masked MVFC images, WTE-15-CD

WTE-15-CD raw (left) and masked (right) MVFC images, for pre-oil (Mixing A, T = 60), oiled (Mixing B, T = 0) and post-oil conditions (mixing B, T = 5).

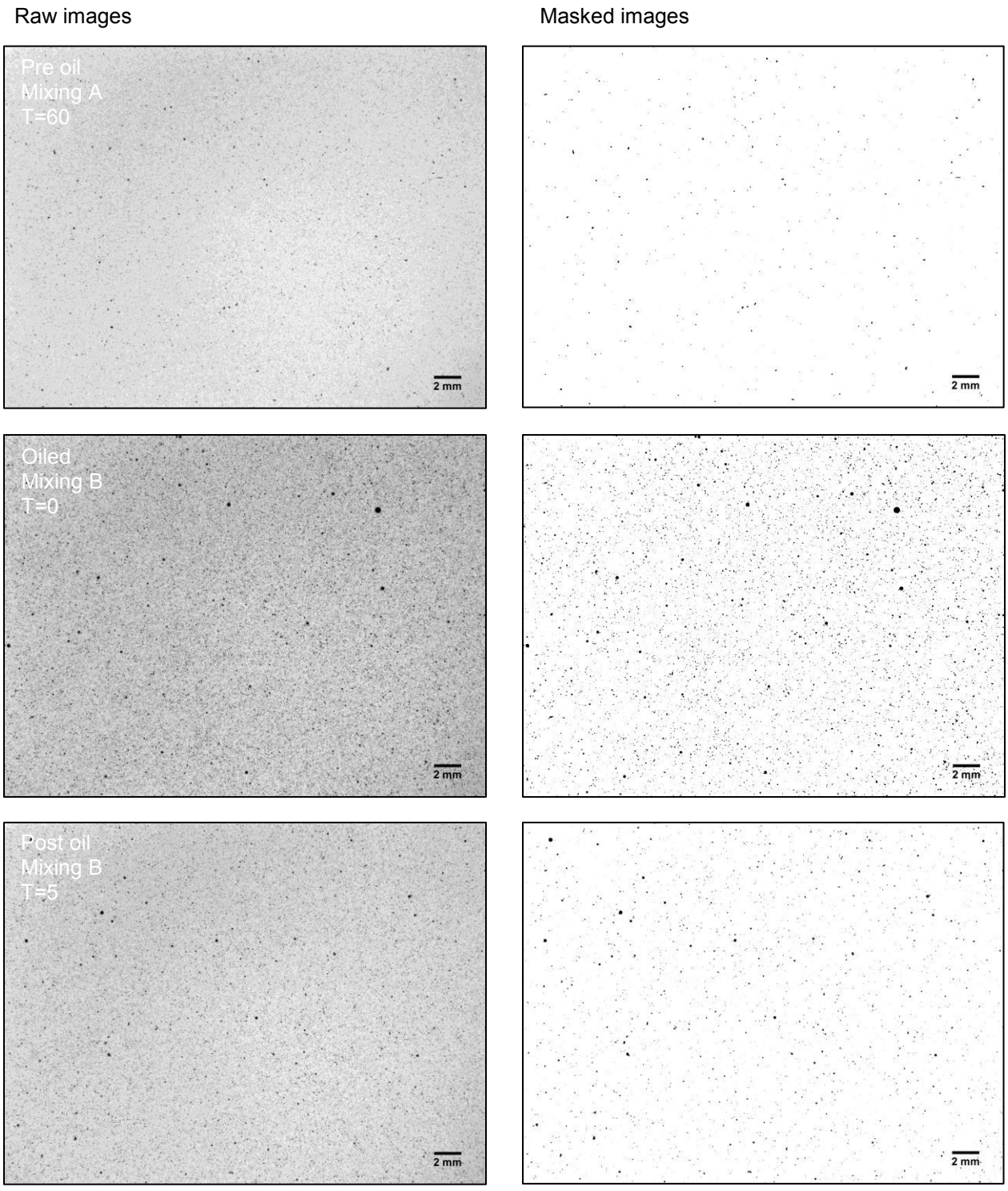

Figure 8: Raw and masked MVFC images, WTE-17-CD

WTE-17-CD raw (left) and masked (right) MVFC images, for pre-oil (Mixing A, T = 60), oiled (Mixing B, T = 0) and post-oil conditions (mixing B, T = 5).

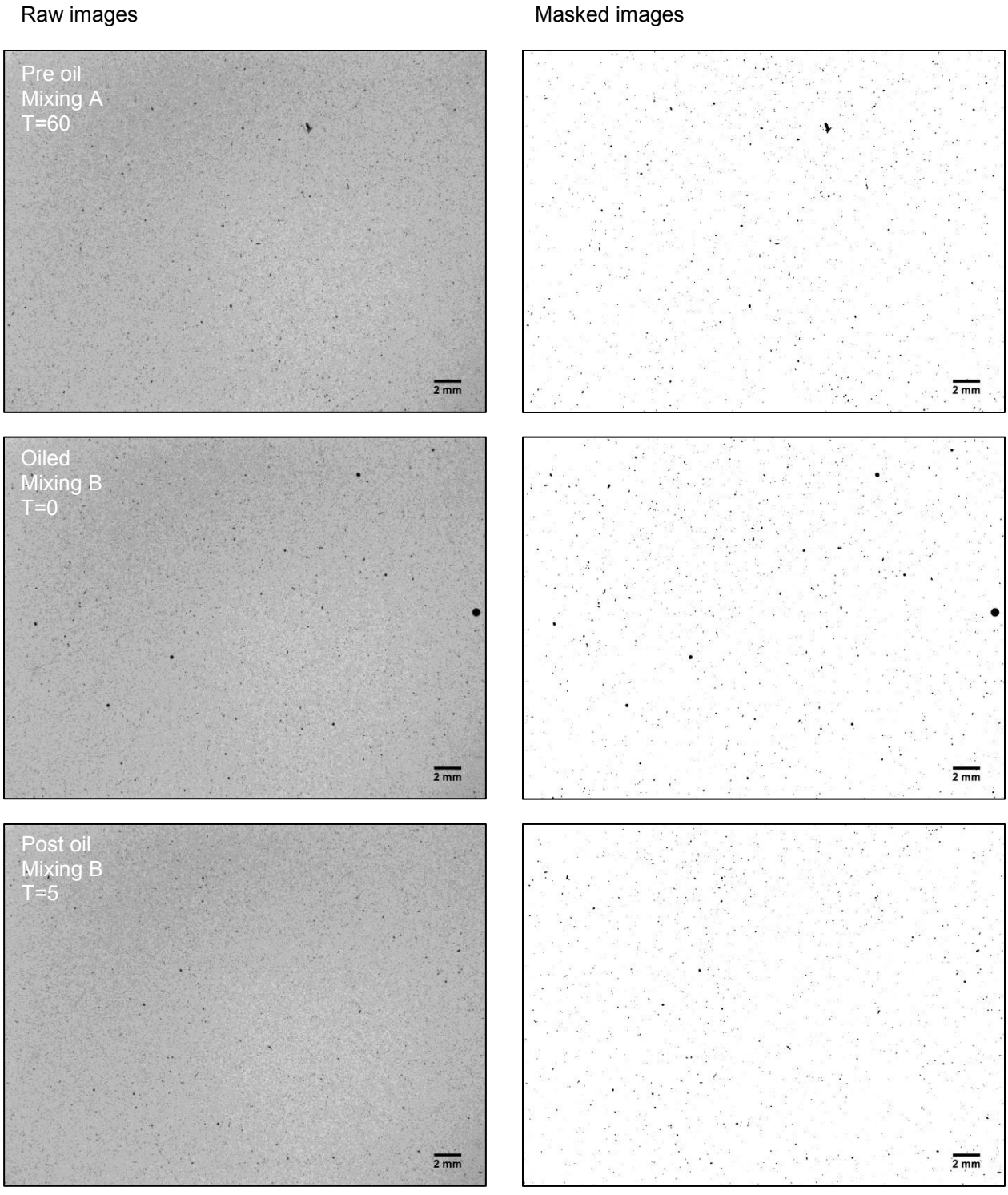

Figure 9: Raw and masked MVFC images, WTE-18-NCD

WTE-18-NCD raw (left) and masked (right) MVFC images, for pre-oil (Mixing A, T = 60), oiled (Mixing B, T = 0) and post-oil conditions (mixing B, T = 5).

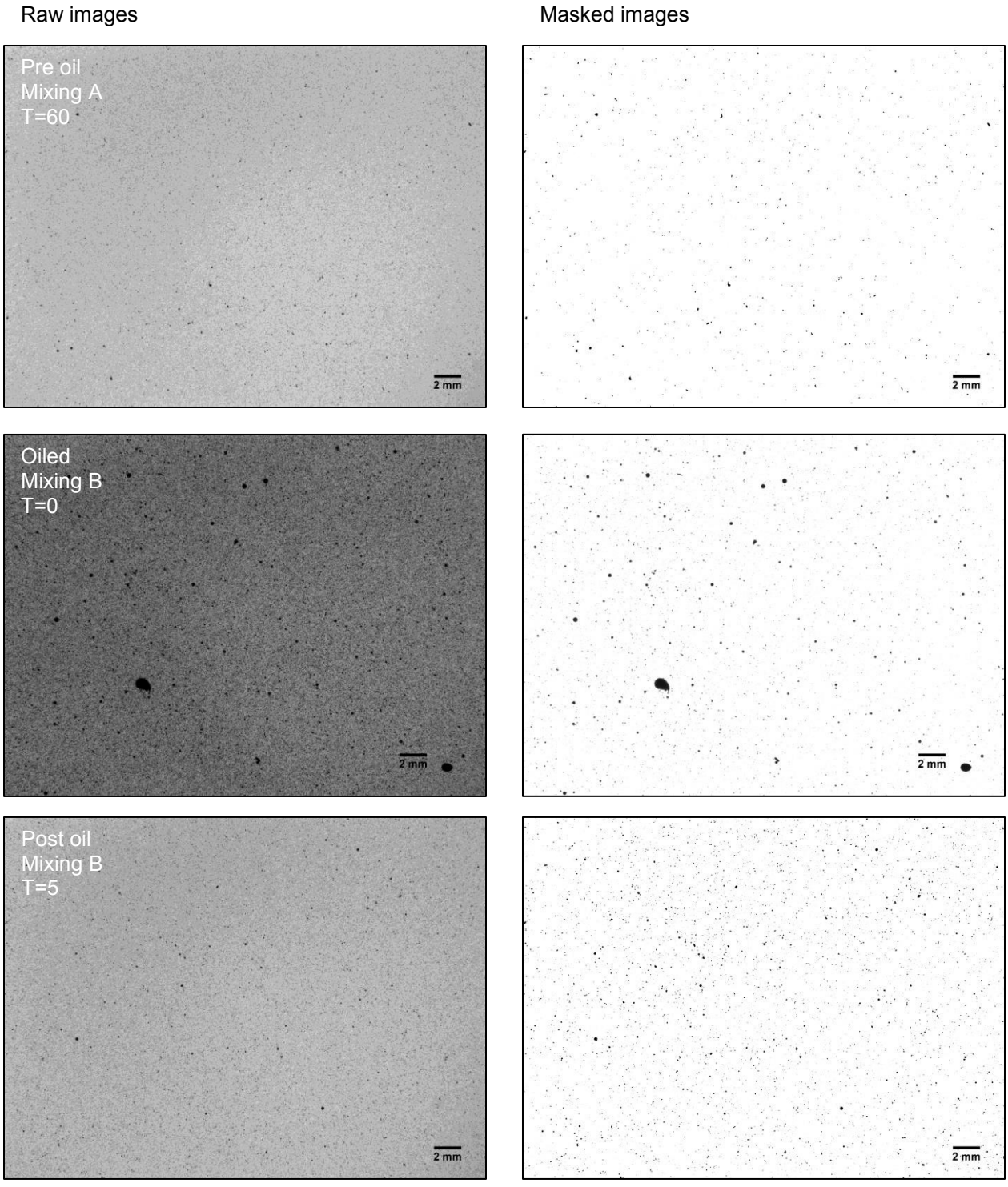

Figure 10: Raw and masked MVFC images, WTE-19-CD

WTE-19-CD raw (left) and masked (right) MVFC images, for pre-oil (Mixing A, T = 60), oiled (Mixing B, T = 0) and post-oil conditions (mixing B, T = 5).

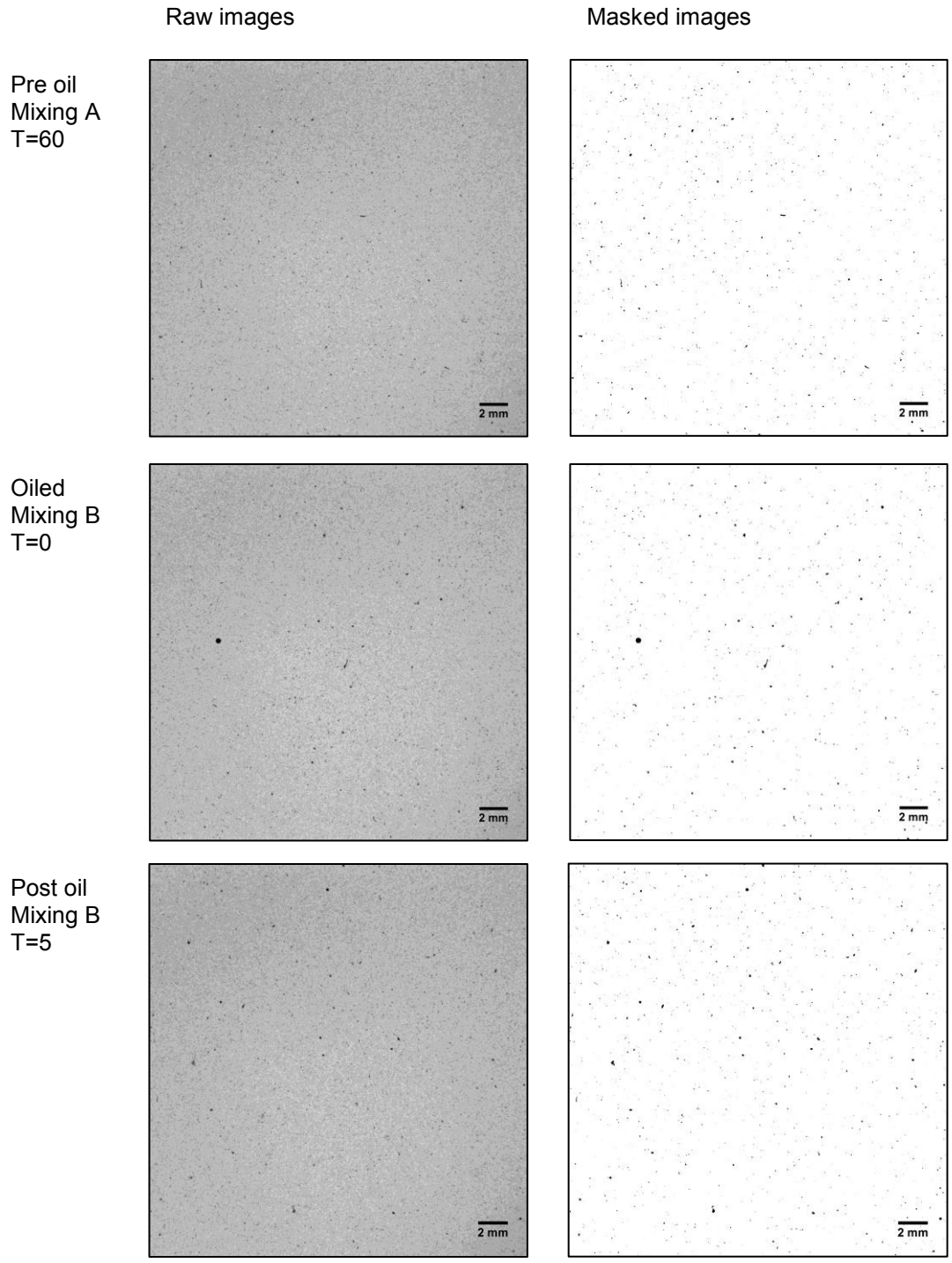

Figure 11: Raw and masked MVFC images, WTE-20-NCD

WTE-20 raw (left) and masked (right) MVFC images, for pre-oil (Mixing A, T = 60), oiled (Mixing B, T = 0) and post-oil conditions (mixing B, T = 5). WTE-20 images were cropped to exclude obstructions on the lens, resulting in smaller images.

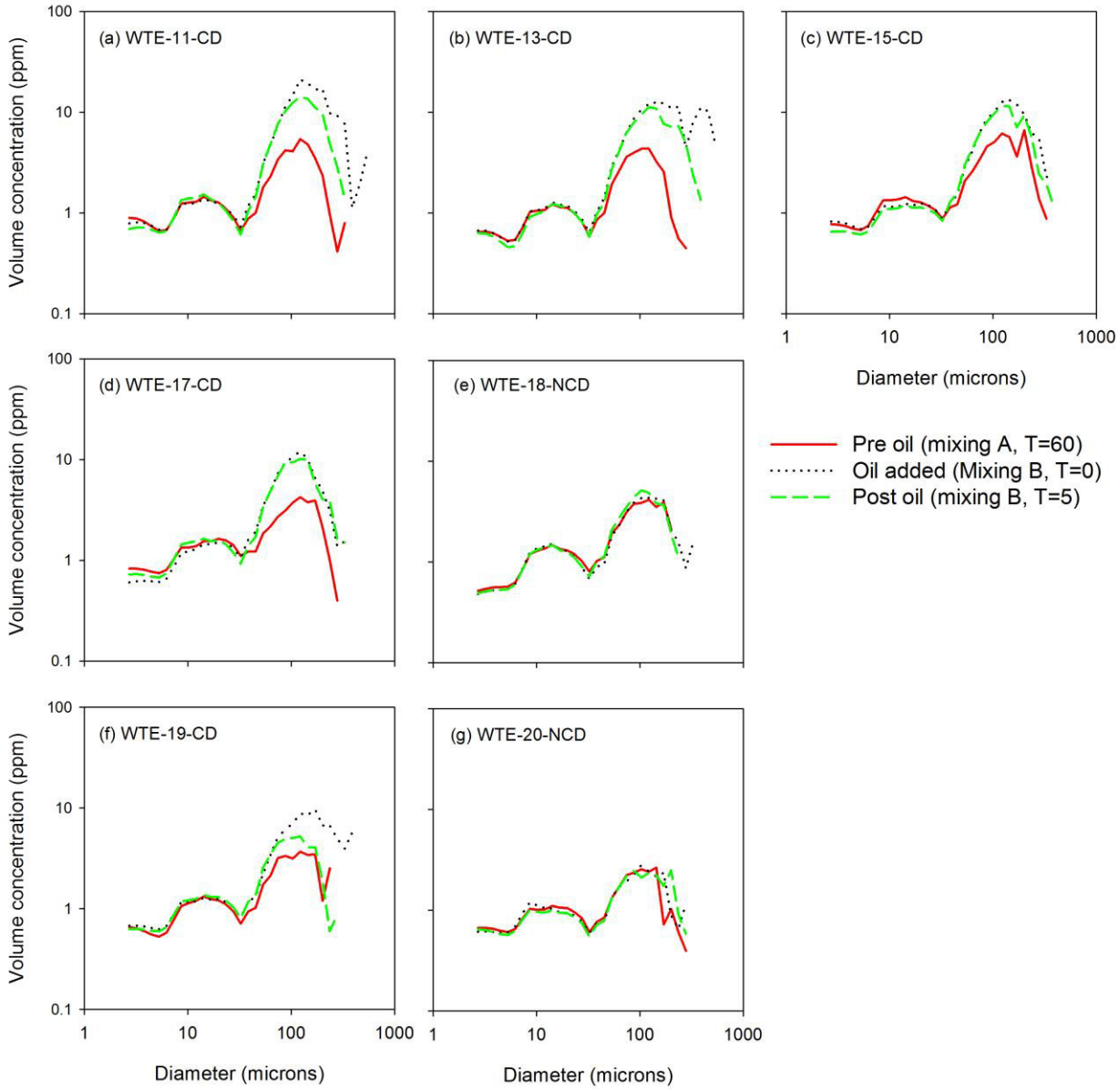

Figure 12: Merged particle size spectra before, during and immediately after the addition of oil

A comparison of merged particle size spectra for warmer water (> 10°C) wave tank experiments, characterizing the end of the first mixing phase (Mixing A), the addition of oil, and start of the second mixing phase (Mixing B). Waves were stopped and oil was added to the wave tank between T = 60 (mixing A) and T = 0 (mixing B). Data are expressed as the log of the volume concentration (ppm) versus the log of particle diameter (µm)

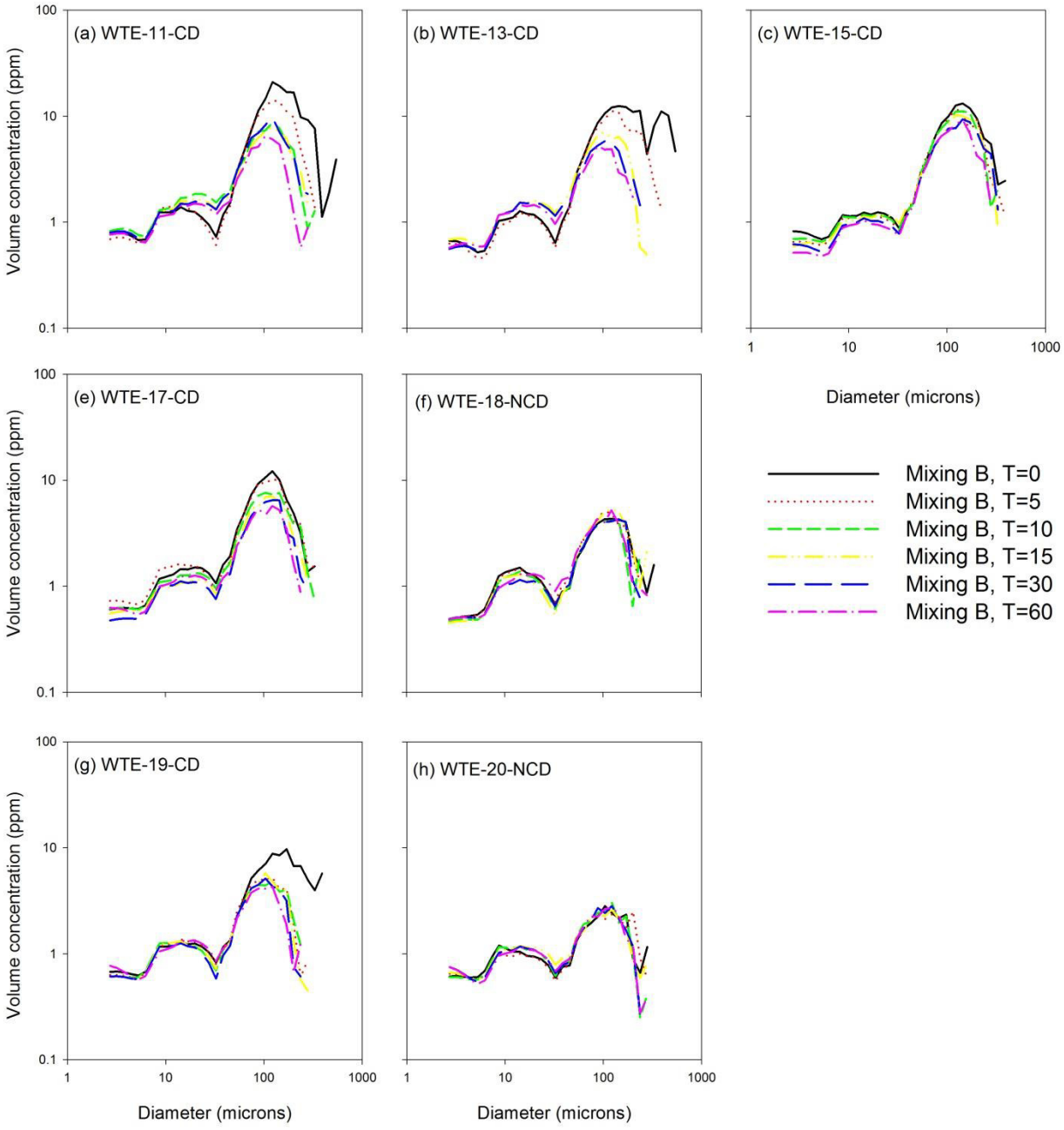

Figure 13: Merged particle size spectra following the addition of oil (Mixing B)

A comparison of merged particle size spectra throughout the second mixing phase (Mixing B), for warmer water (> 10°C) wave tank experiments. Waves were stopped and oil was added to the wave tank between T = 60 (mixing A) and T = 0 (mixing B); subsequent particle size curves are shown at 5 and 15 minute increments. Data are expressed as the log of the volume concentration (ppm) versus the log of particle diameter (µm)

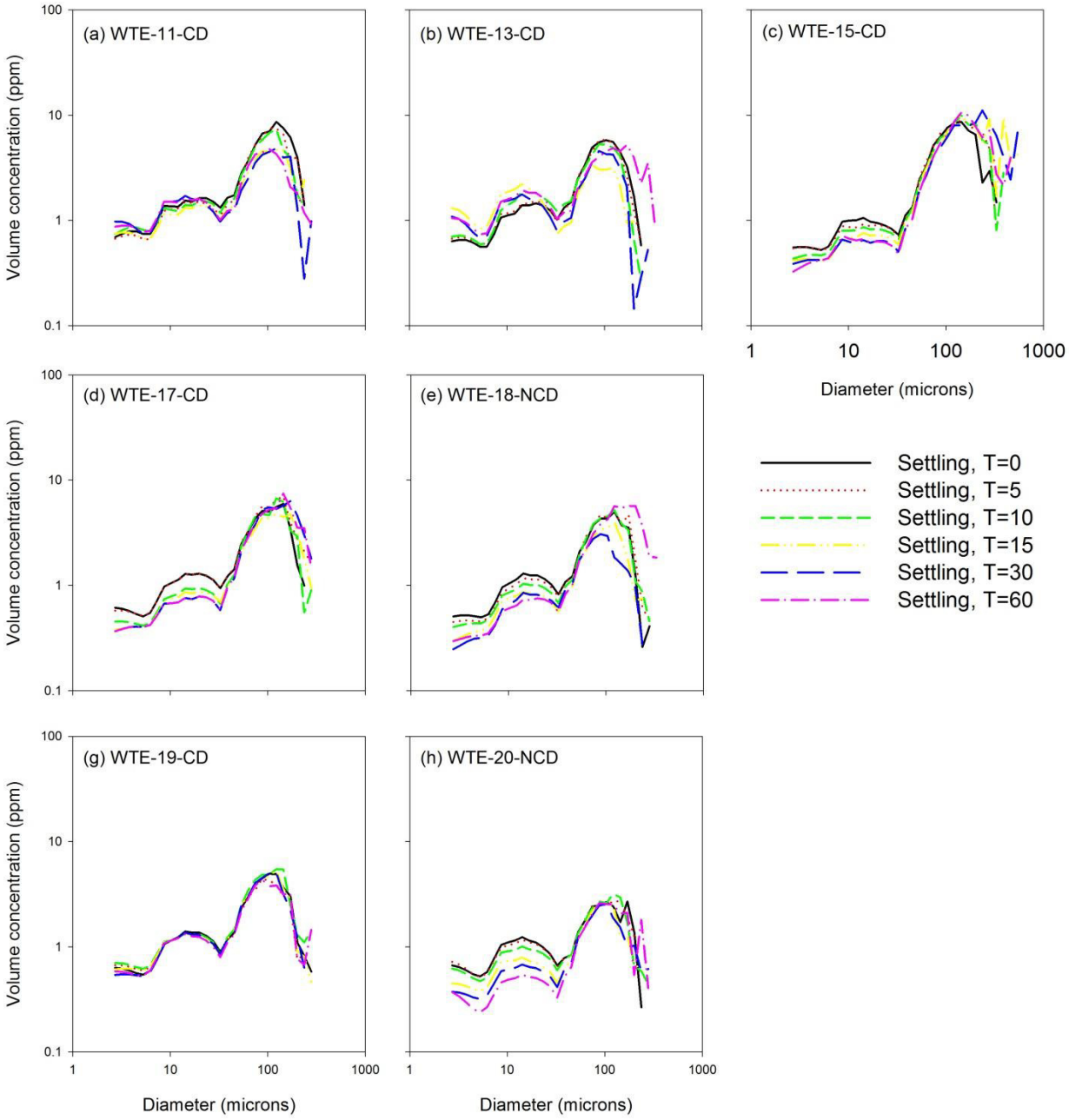

Figure 14: Merged particle size spectra following the cessation of wave energy (Settling)

A comparison of merged particle size spectra during settling phases from warmer water (> 10°C) wave tank experiments. Waves were turned off prior to the beginning of this phase (T=0); subsequent particle size curves are shown at 5 and 15 minute increments.

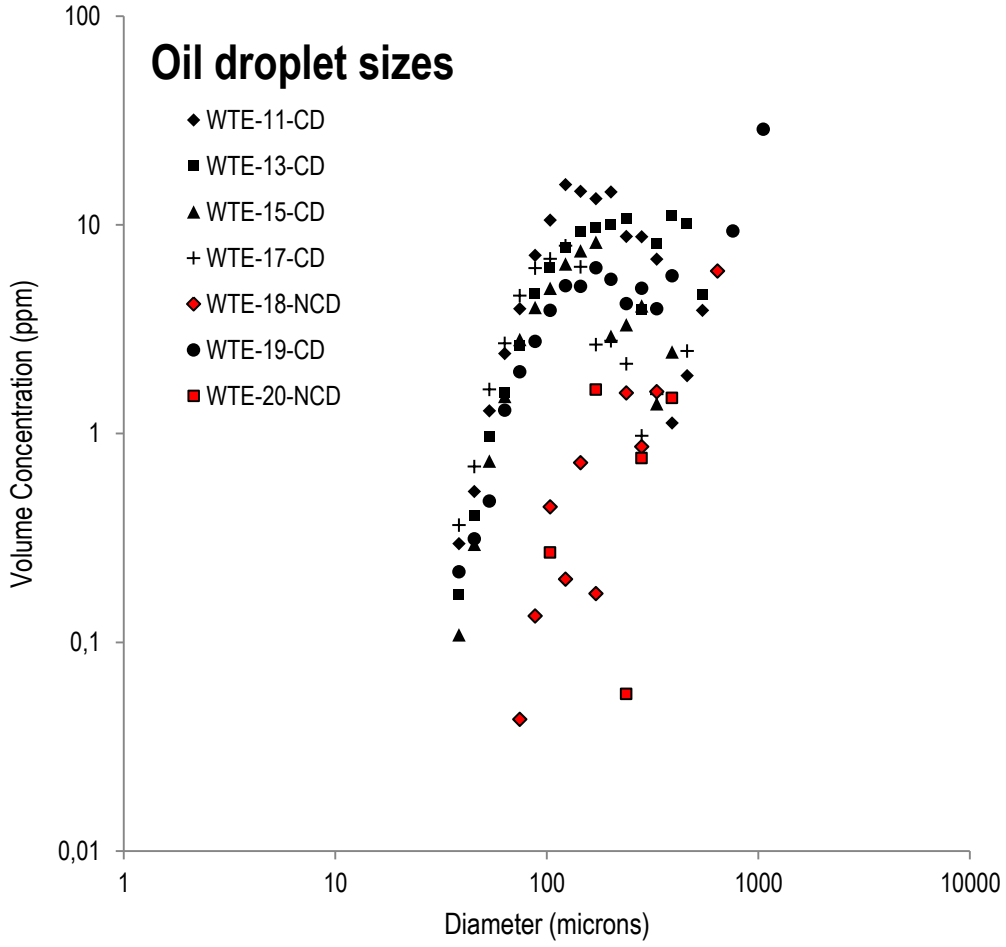

Figure 15: Oil droplet sizes

The size of suspended oil droplets, plotted as the log of volume concentration (ppm) in each size class versus particle diameter (µm). Droplet size was derived from subtraction of MVFC imagery captured pre- and post-oil. Non-chemically dispersed (NCD) experiments are shown in red, and chemically dispersed conditions in black.

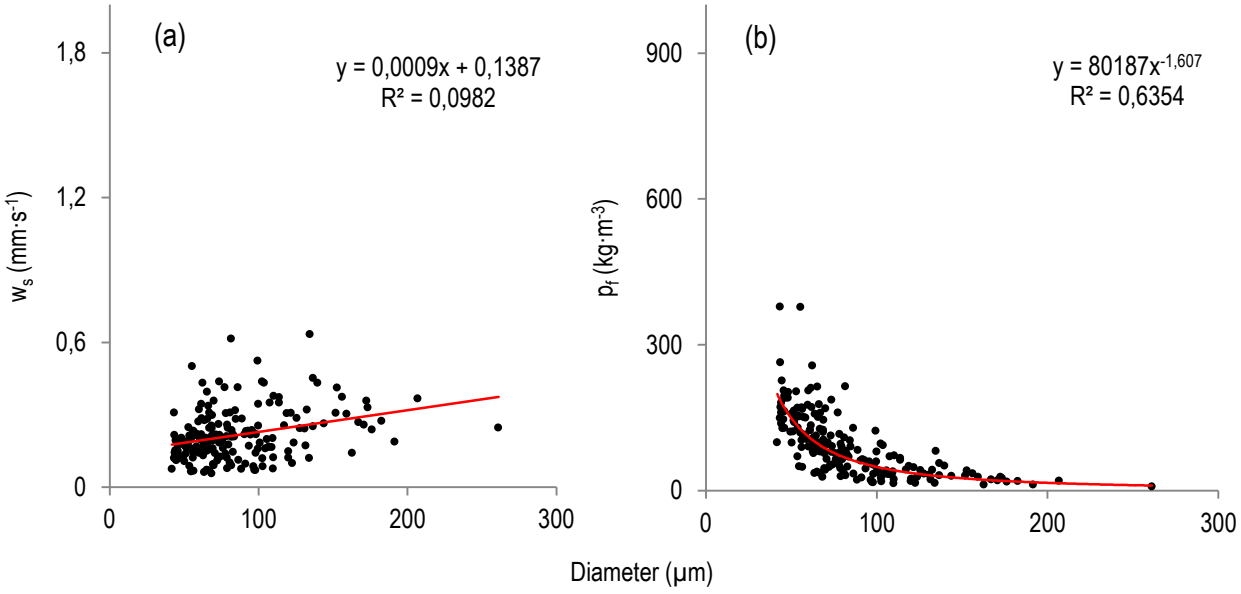

Figure 16: Size-settling relationships, WTE-13-CD

Plots of particle diameter (µm) versus settling velocity (w_s) (mm·s^{-1}) and effective particle density (ρ_f) (kg·m^{-3}), for chemically dispersed experiment WTE-13, fitted to (a) linear and (b) power law models.

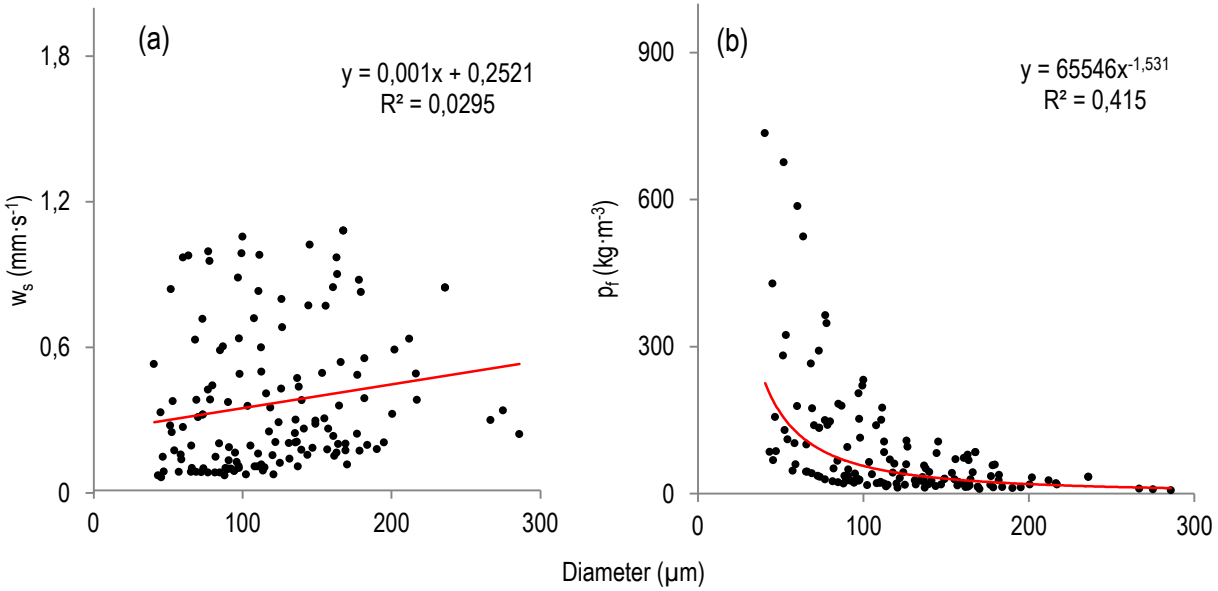

Figure 17: Size-settling relationships, WTE-16-NCD

Plots of particle diameter (µm) versus settling velocity (w_s) (mm·s^{-1}) and effective particle density (ρ_f) (kg·m^{-3}), for non-chemically dispersed experiment WTE-15, fitted to (a) linear and (b) power law models.

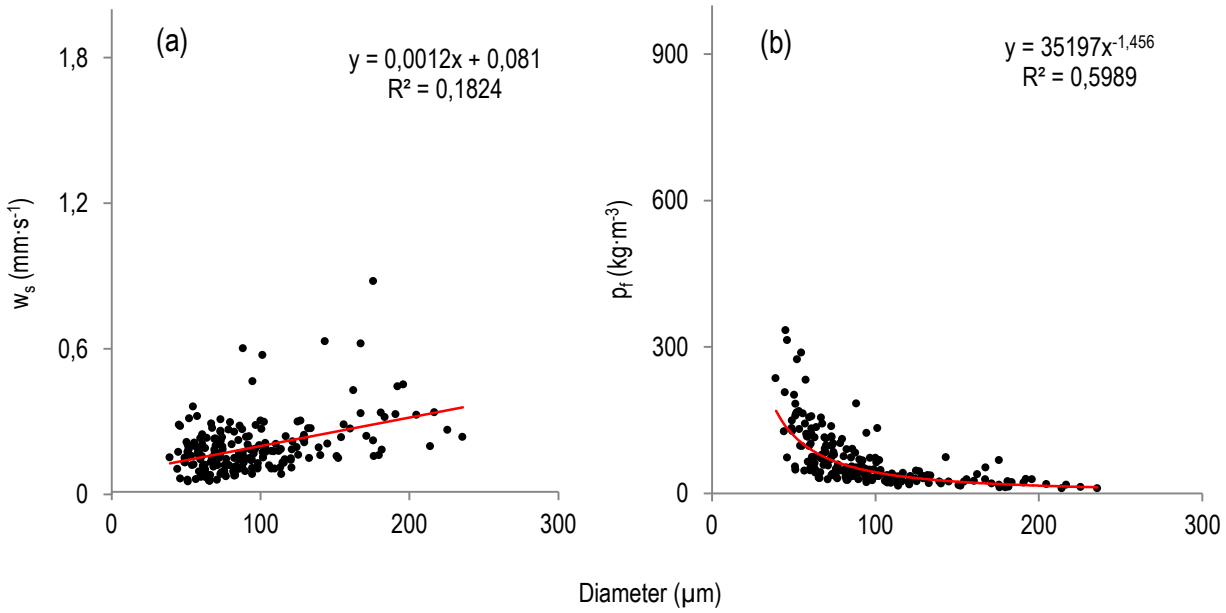

Figure 18: Size-settling relationships, WTE-17-CD

Plots of particle diameter (µm) versus settling velocity (w_s) (mm·s^{-1}) and effective particle density (ρ_f) (kg·m^{-3}), for chemically dispersed experiment WTE-17, fitted to (a) linear and (b) power law models.

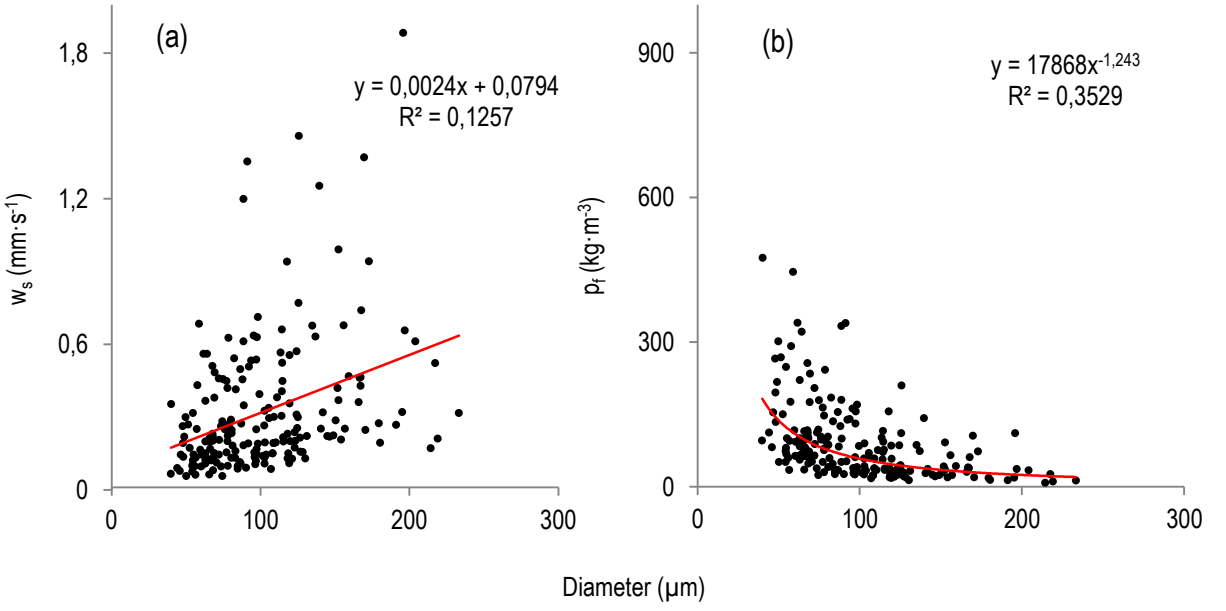

Figure 19: Size-settling relationships, WTE-18-NCD

Plots of particle diameter (µm) versus settling velocity (w_s) (mm·s^{-1}) and effective particle density (ρ_f) (kg·m^{-3}), for non-chemically dispersed experiment WTE-18, fitted to (a) linear and (b) power law models.

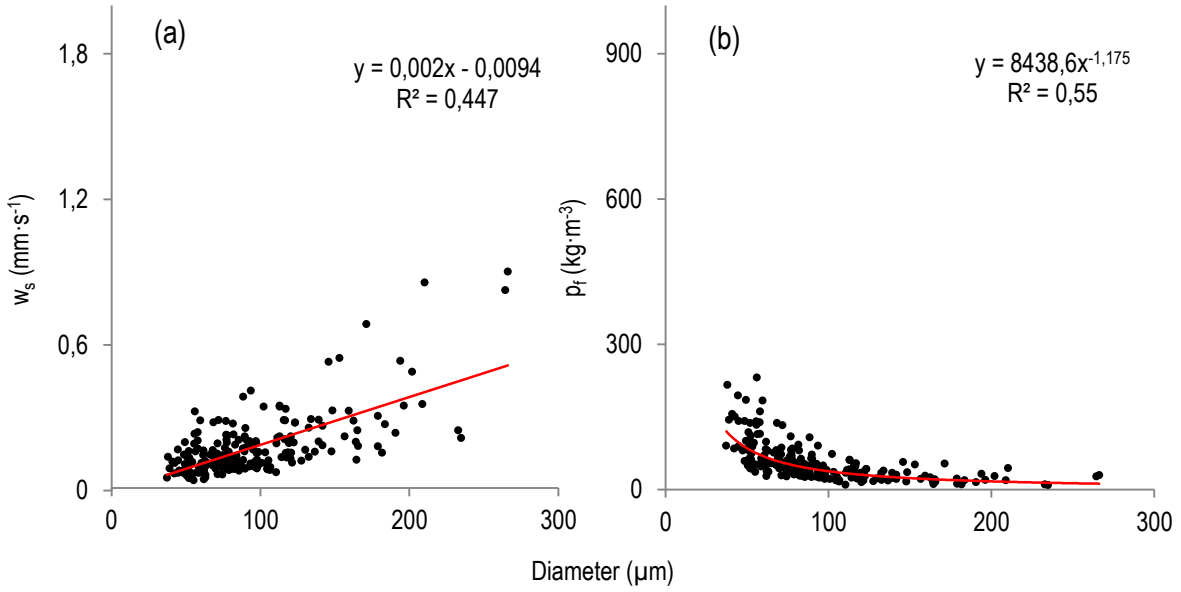

Figure 20: Size-settling relationships, WTE-19-CD

Plots of particle diameter (µm) versus settling velocity (w_s) ($mm \cdot s^{-1}$) and effective particle density (ρ_f) ($kg \cdot m^{-3}$), for chemically dispersed experiment WTE-19, fitted to (a) linear and (b) power law models.

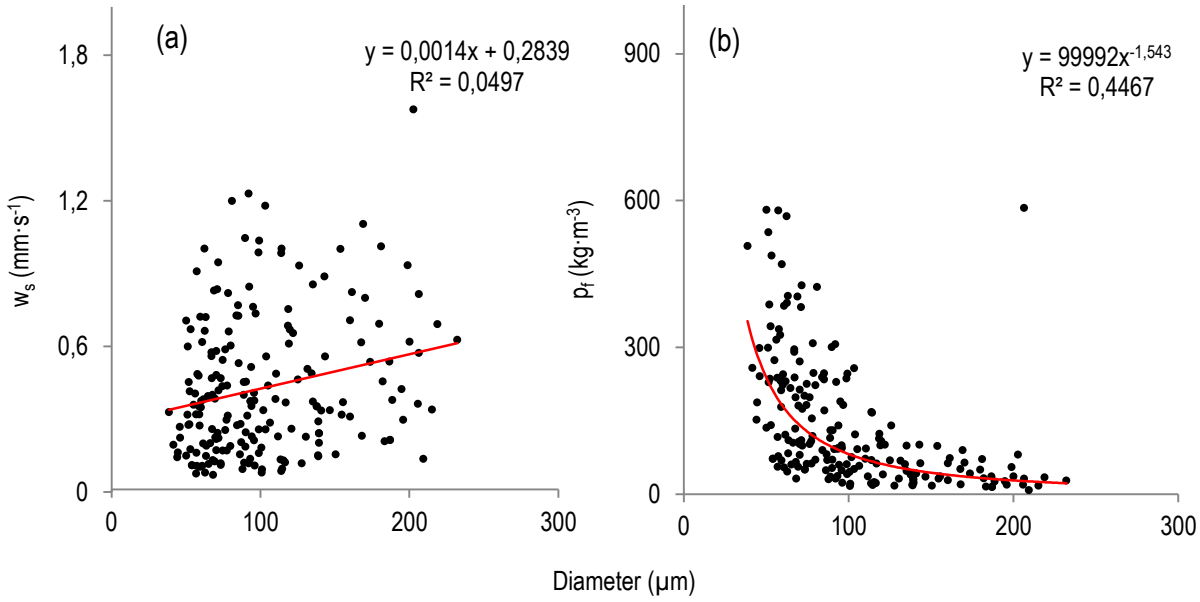

Figure 21: Size-settling relationships, WTE-20-NCD

Plots of particle diameter (µm) versus settling velocity (w_s) ($mm \cdot s^{-1}$) and effective particle density (ρ_f) ($kg \cdot m^{-3}$), for non-chemically dispersed experiment WTE-20, fitted to (a) linear and (b) power law models.

Non-dispersed experiments			
Experiment	**Size (μm)**	**Settling velocity ($mm \cdot s^{-1}$)**	**Density ($kg \cdot m^{-3}$)**
WTE-16-NCD	120.86	0.3705	87.64
WTE-18-NCD	100.59	0.3195	88.72
WTE-20-NCD	101.93	0.4287	140.13
Means:	107.79	0.3729	105.50
Dispersed experiments			
WTE-13-CD	85.31	0.2163	92.53
WTE-17-CD	95.99	0.1967	88.93
WTE-19-CD	93.87	0.1756	64.42
Means:	91.72	0.1962	81.96

Table 3: Size-settling summary

Summary of size, settling velocity and effective particle density analysis on images collected with the SVS-MVFC at 145 cm depth (position D). Mean per-experiment values of particle size (μm), settling velocity ($mm \cdot s^{-1}$) and effective particle density ($kg \cdot m^{-3}$) are shown, grouped by the presence of chemical dispersant (CD = chemically dispersed, NCD = non-chemically dispersed). Mean values for chemically dispersed and non-chemically dispersed groupings are also shown.

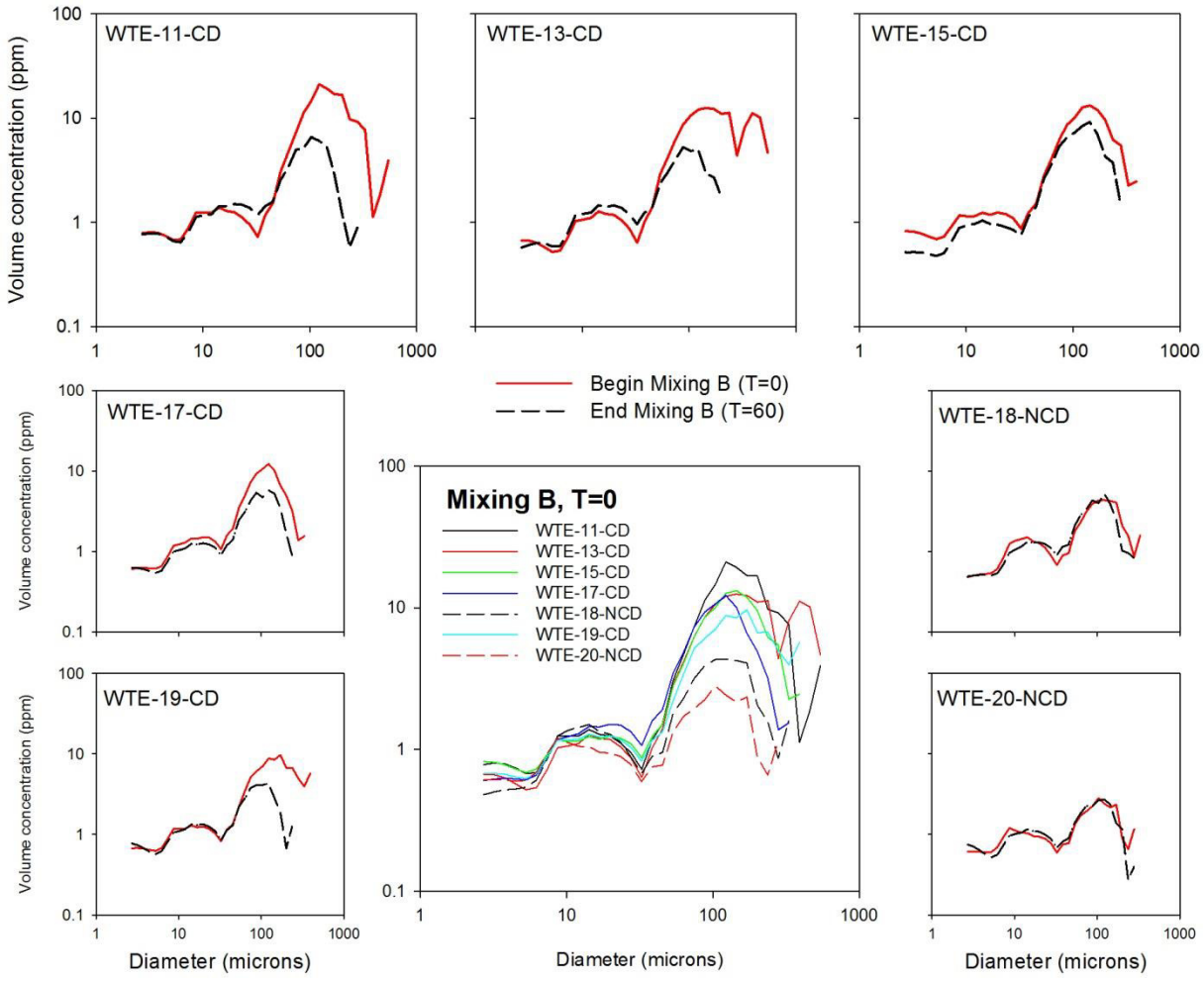

Figure 22: Merged grain size spectra, Mixing B (T=0)

Edges: Merged grain size spectra at the beginning (T=0) and ending (T=60) of the second mixing phase (Mixing 'B'), plotted as the log of volume concentration (ppm) versus the log of particle diameter (µm). Center: An overlain comparison of merged grain size spectra at the beginning of Mixing B, or immediately following the addition of oil (NCD, dashed lines), or oil and dispersant (CD, solid lines). Again, data are plotted as the log of volume concentration (ppm) versus the log of particle diameter (µm).

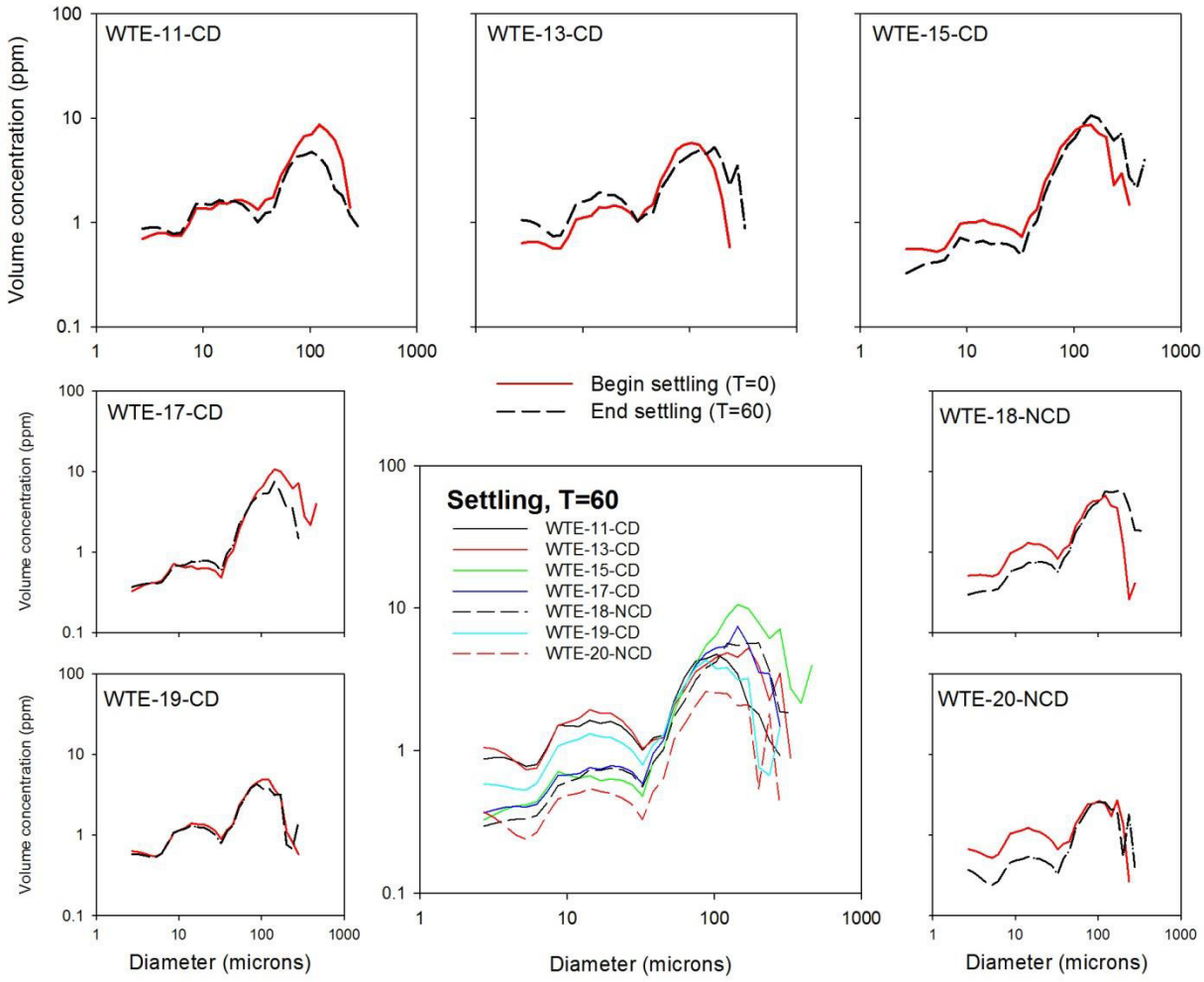

Figure 23: Merged grain size spectra, Settling (T=60)

Edges: Merged grain size spectra at the beginning (T=0) and ending (T=60) of the settling phase, plotted as the log of volume concentration (ppm) versus the log of particle diameter (µm). Center: An overlain comparison of merged grain size spectra from the conclusion of settling phases, plotted as the log of volume concentration (ppm) versus the log of particle diameter (µm). Chemically dispersed (CD) results are shown with solid lines, and non-chemically dispersed (NCD) with dashed.

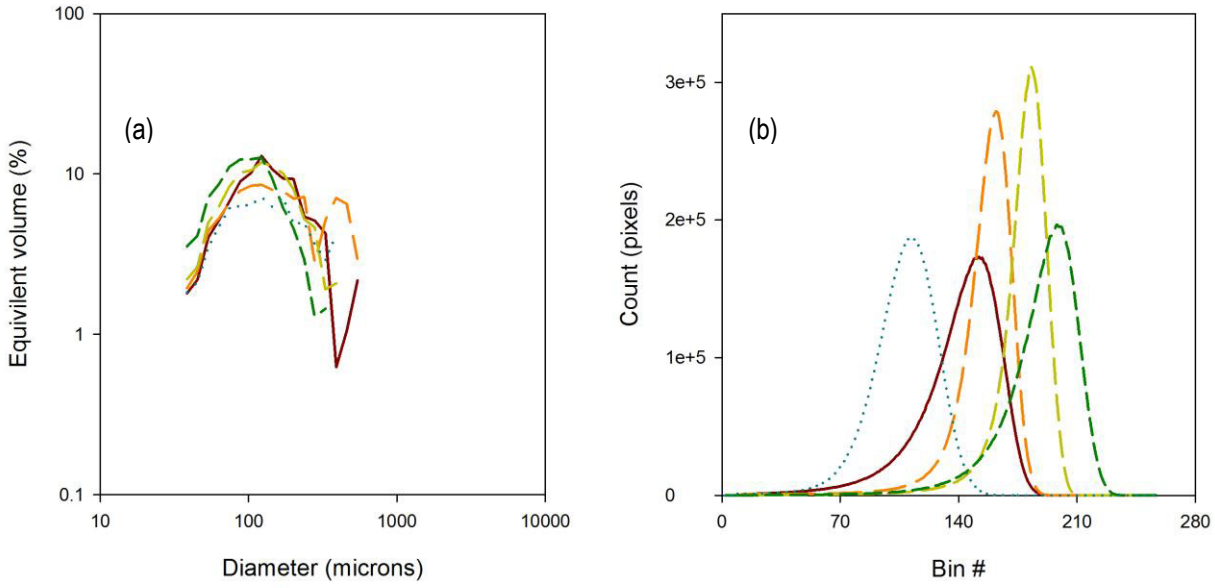

Expt. ID	Image ID	E
WTE-11-CD	P-140612-105859-00257	6.47
WTE-13-CD	P-140624-105129-00232	5.84
WTE-15-CD	P-141007-103603-00221	5.71
WTE-17-CD	P-141009-100336-00257	6.31
WTE-19-CD	P-140616-102325-00178	6.24

Figure 24: Particle size spectra and entropy results

Particle size spectra derived from MVFC images collected immediately after the addition of dispersant (a) are plotted as the log of equivalent volume (%) versus the log of particle diameter (μm). The full greyscale spectra following entropy analysis (b) highlights variability in particle size distributions, which are related to dispersant efficiency in each experiment. Inset table: Dimensionless entropy values (*E)* are shown with corresponding image and wave tank experiment.

	WTE-11	WTE-13	WTE-15	WTE-16	WTE-17	WTE-18	WTE-19	WTE-20
% DE at T=60	46.4	53.6	50.4	6.9	63.3	6.4	63.1	13.5
% DE at T=180	24.7	34.1	26.0	5.9	45.1	6.9	74.2	8.4

Table 4: Oil dispersion efficacy

Dispersion efficacy (DE) (%) for wave tank experiments using Douglas Channel sediments with AWB/CLB dilbit treated with/without Corexit 9500. Note that an efficacy of 100% would indicate that all of the oil added to the tank was dispersed into the water column. Dispersion efficacy from 2 points during each experiment: T = 60 (mixing B) and T = 180 (end of settling).

	Mean wind speed during each experiment (km/h)	Wind speed during dispersant application (km/h)
WTE-11-CD	16.0	20
WTE-13-CD	14.8	16
WTE-15-CD	11.8	15
WTE-17-CD	22.0	25
WTE-19-CD	7.0	4

Table 5: Wind conditions during wave tank experiments

Bedford Basin wind conditions during chemically dispersed wave tank experiments. The wave tank facility is directly adjacent to Bedford Basin, where weather conditions are monitored by Environment Canada. Mean wind speed (km/h) for the duration of each experiment, as well as the hourly value corresponding with dispersant applications, are shown here.

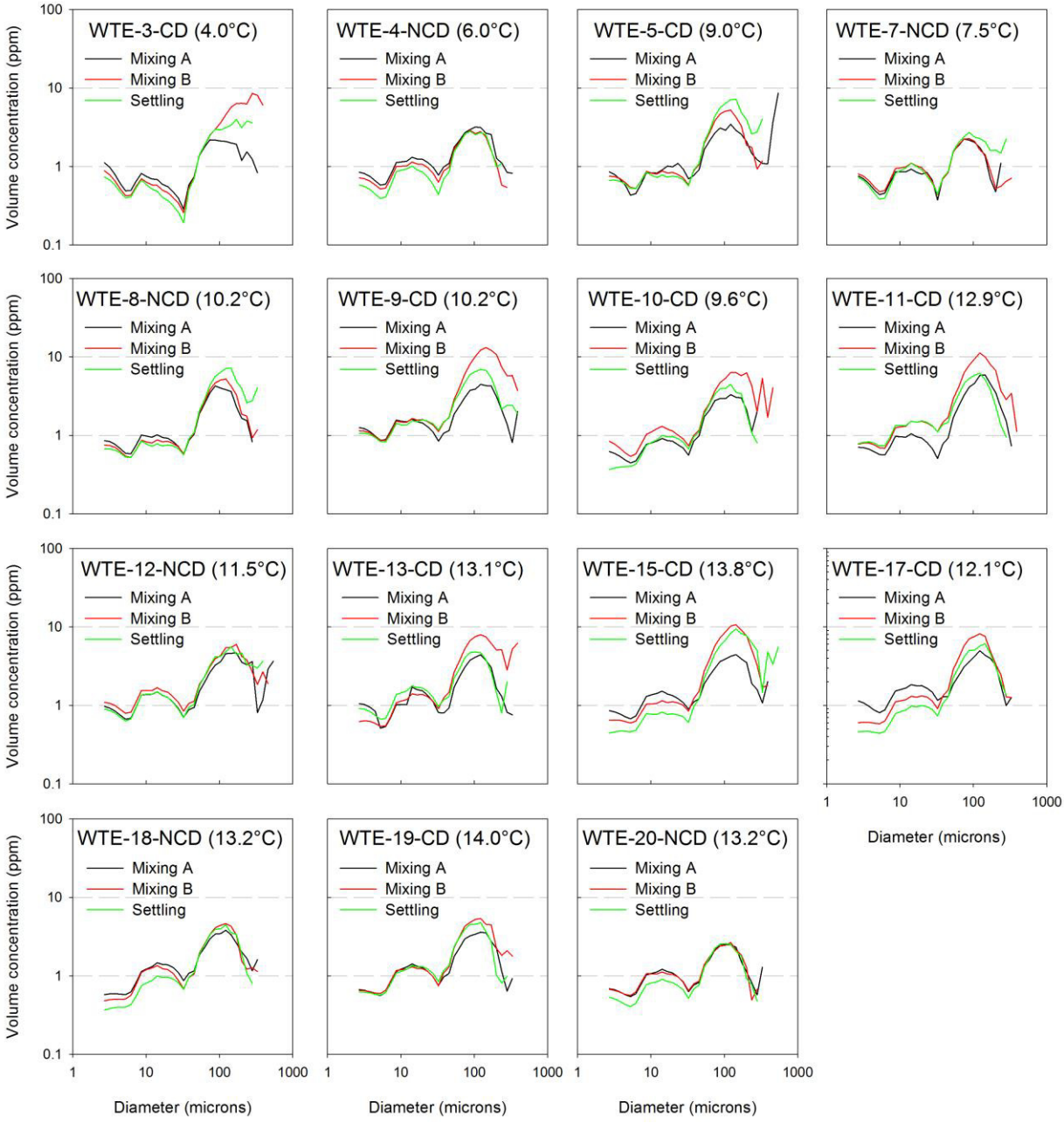

Figure 25: Averaged merged particle size spectra, all experiments

Merged particle size spectra, averaged over the three phases of interest for cold (<10°C) and warm (>10°C) water experiments. Data are plotted as the log of volume concentration (ppm) versus the log of particle diameter (microns). Experiment name, including condition (CD = chemically dispersed; NCD = non-chemically dispersed) and water temperature are shown in each panel.

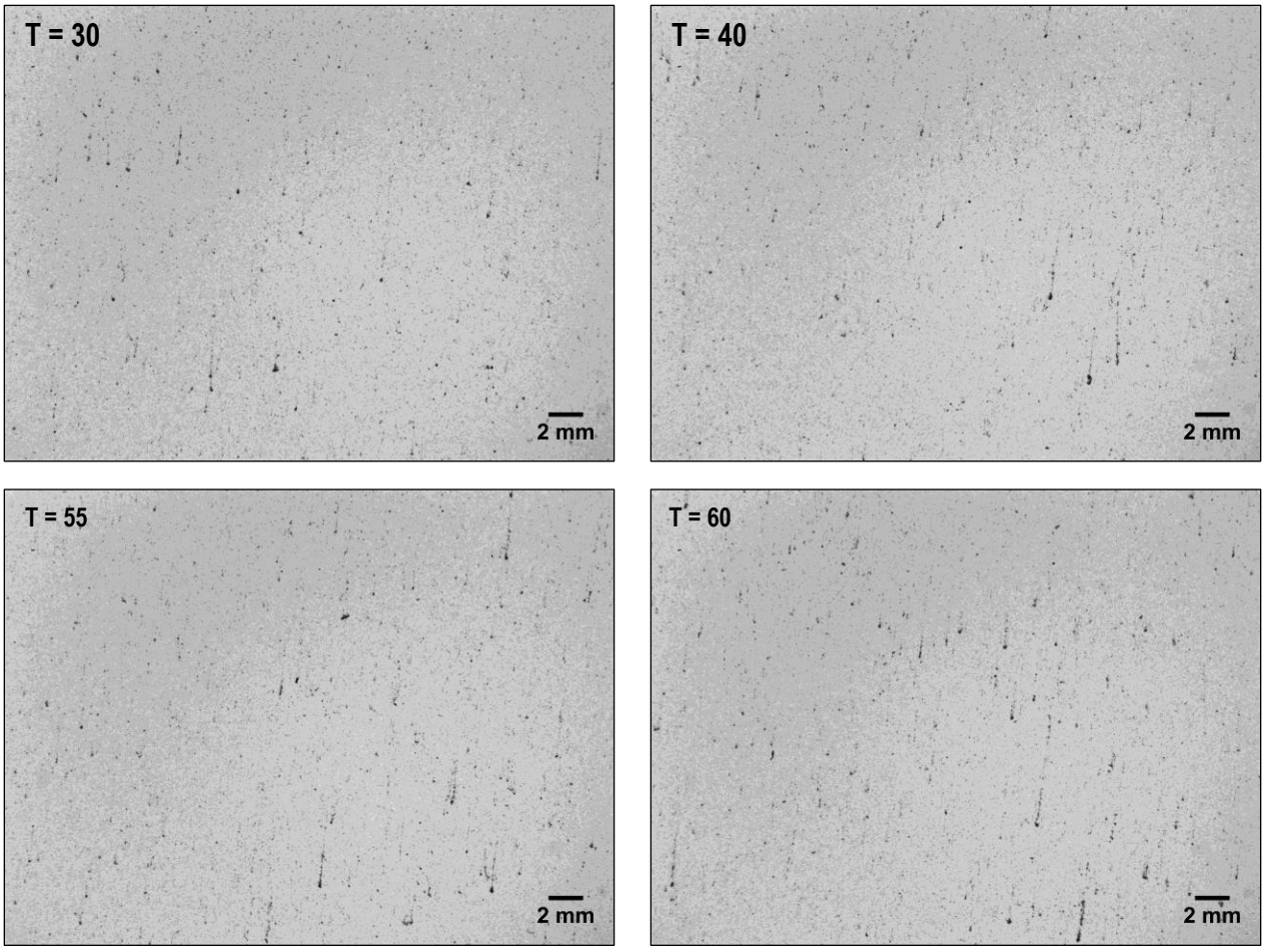

Figure 26: Elongated particles settling during WTE-15-CD

Particle shape and size were notably different during WTE-15-CD. Images collected during the mid-to-late settling phase (T=30+) showed the development of elongated, comet-like particles. Raw greyscale images captured with the MVFC (position B, 35 cm depth) are shown; image capture time is indicated, in minutes relative to the start of the settling phase.

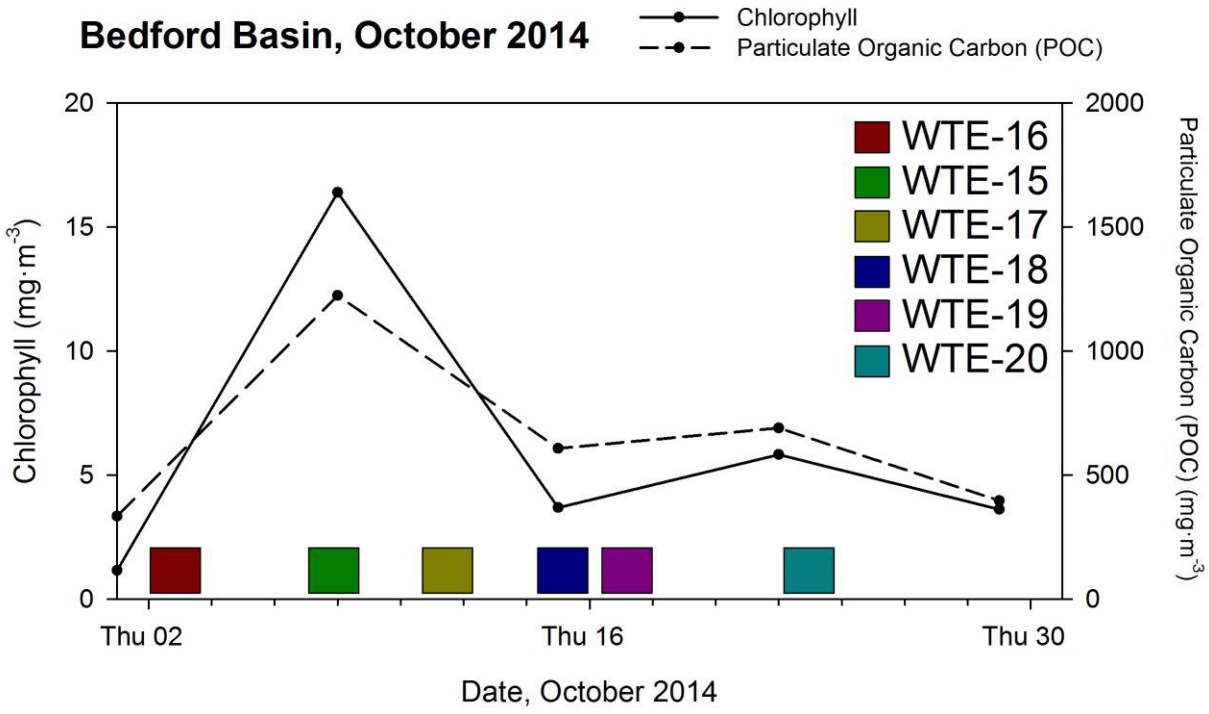

Figure 27: Elevated chlorophyll and particulate organic carbon

Experiment water was pumped into the wave tank from the adjacent Bedford Basin. Weekly water quality data from the Bedford Basin, derived from Niskin water samples, indicate elevated chlorophyll and particulate organic carbon levels during the experiment WTE-15-CD.

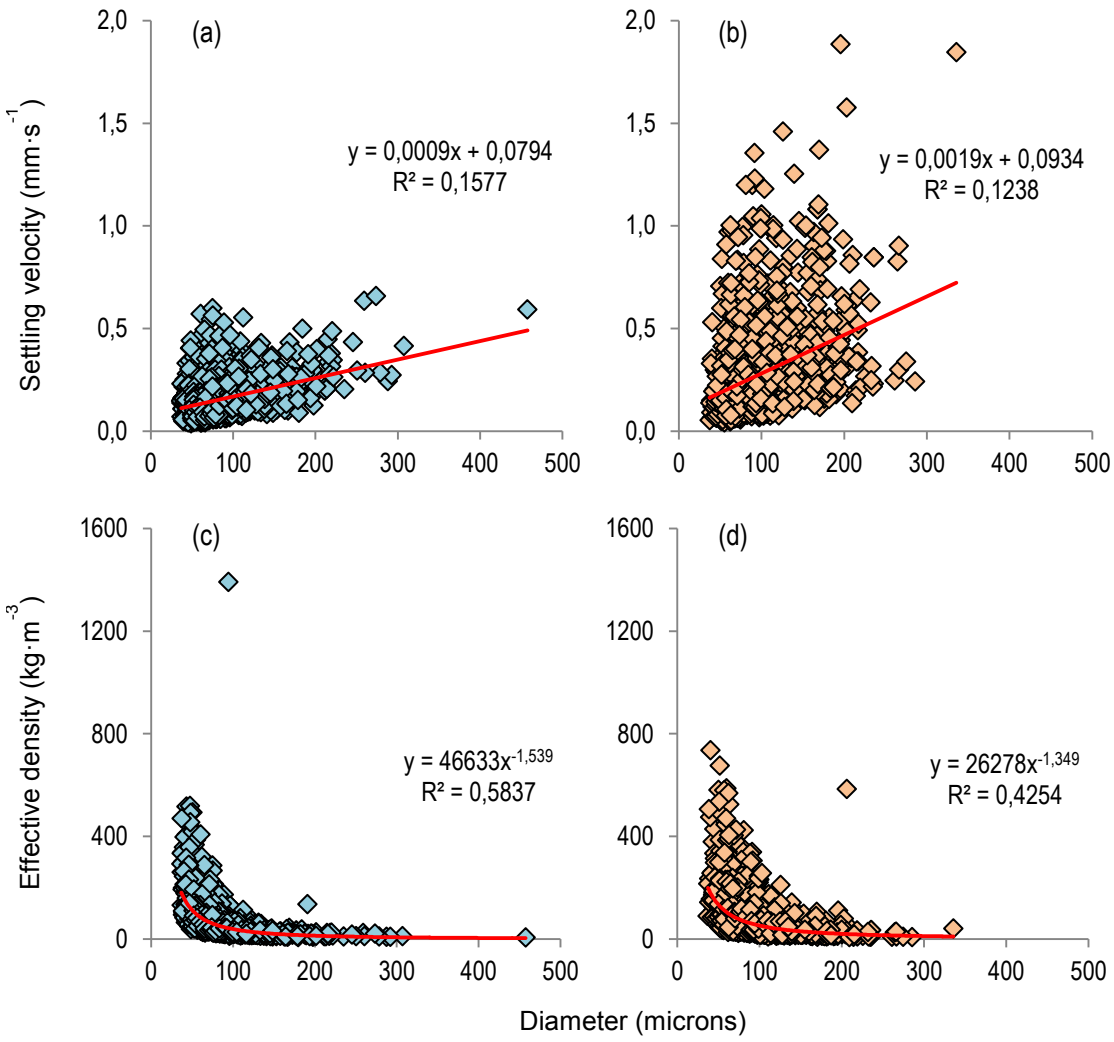

Figure 28: Size versus settling and effective density, colder and warmer water

Size-settling and size-density relationships for eight colder water (< 10°C) experiments (panels a, c) and eight warmer water (>10°C) experiments (panels b, d) are shown, plotted as settling velocity ($mm \cdot s^{-1}$) or particle density ($kg \cdot m^{-3}$) versus particle diameter (microns). Data are fitted to linear (a,b) and power law models (c,d).

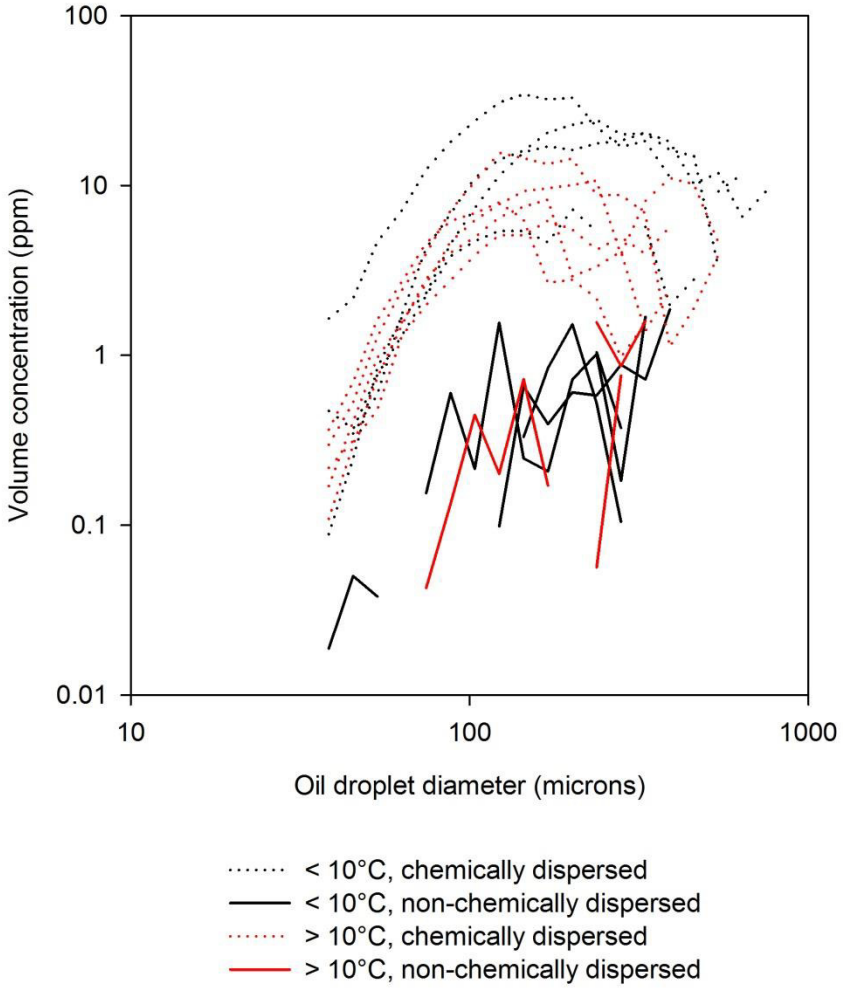

Figure 29: Oil droplet sizes, colder and warmer water

Oil droplet diameters for colder (<10°C) and warmer (>10°C) water wave tank experiments are shown, plotted as the log of volume concentration (ppm) versus the log of oil droplet diameter (microns). Chemically dispersed experiments are shown with dashed lines, while non-chemically dispersed experiments are shown with solid lines.